An experimental investigation to the constitutive behaviour of brain tissue

An Experimental Investigation to the Constitutive Behaviour of Brain Tissue

J.H. Meulman

CIP-Data Koninklijke Bibliotheek, The Hague
Meulman, J.H.
An experimental investigation to the constitutive behaviour of brain tissue
J.H. Meulman - Eindhoven: Stan Ackermans Institute
Technological designer course Computational Mechanics
With references
ISBN 90-5282-638-2
Subject headings: biomechanics / brain tissue / time-temperature superposition

WFW 96.059

Summary

As part of the research program "Head Injuries" mathematical models are developed to similate reponses of the human head upon impacts (characteristic duration between 1–50 ms). The mechanical properties of various materials are necessary to develope these models. A literature study did not result in reliable data to describe the constitutive behaviour of brain tissue. Therefore torsional shear experiments were performed with brain tissue on the RFS II (for frequencies between 0.159 and 15.9 Hz). The brain tissue was considered as a linear viscoelastic isotropic material. The behaviour was shown to be physical linear under conditions, indicated to be geometrically linear. To obtain information about the constitutive behaviour of brain tissue at frequencies relevant for impacts (20–1000 Hz) the application of the time/temperature superposition was investigated. With help of the generalised Maxwell model for solids and conform experience, four criteria were derived. These criteria were satisfied. Thus no arguments were found that reject the use of the principle upon brain tissue. Sets of isothermal characteristics for the relaxation modulus, the dynamic modulus and the loss angle (temperature varied between 7 and 38°C) were used to construct master curves. These curves describe the mechanical behaviour of brain tissue for frequencies between 1 and 10^6 Hz. The generalised Maxwell model for solids was fitted upon these master curves. Comparison of the results of the relaxation and dynamic experiments showed that the differences between the calculated fits and the mastercurves were smaller than the errors induced by the application of the time/temperature superposition principle.

The number of samples, used in the experiments, is too small to draw final conclusions about the applicability of the time/temperature superposition principle upon brain tissue. To obtain more certianty the temperature control system has to be improved. Further, the density has to be known on the used temperature range.

Next, histological investigations has to be performed to get an indication of the structural changes, induced by the storage, the preparation method and the experiments.

The used experimental setup is not suitable to obtain information about anisotropic properties of brain tissue or to estimate inhomogeneous behaviour.

Contents

1 Introduction

1.1 Problem definition

The head is identified as the body area most frequently involved in life-threatening injuries in traffic accidents (ETSC, 1993). Injuries of the human head can be divided in two groups. First, the head and brains can be injured by impacts, deforming the skull and also the brains. The second group are the injuries caused by fast and large rotations or translations of the human head. These movements are regarded responsible for injuries as DAI (Diffuse Axonal Injury) or ASDH (Acute SubDural Hematoma). Victims can be invalid for life or be killed without superficial wounds on their heads. To estimate the chance for these internal wounds, head protection criteria can be used. To draw up these criteria, mechanisms that cause these injuries have to be known.

In cooperation with TNO, Eindhoven University of Technology has started up a research program called 'Head Injuries'. The aim of this project is twofold:

1. The development of an experimentally verified, mathematical model for the human head to obtain a comprehension of the relations between impact conditions and the resulting injuries.

2. To draw up and verify protection criteria on the basis of those relations.

The first step in this program is the development of a finite element model of the human head. With this model the responses of the human head to impacts (characteristic duration between 1–50 ms (Wismans et al., 1994)) can be simulated. To study the need to model the various structures in the human head and the extent of specification, the constitutive behaviour of the separate materials has to be known. Therefore a project was started to examine the constitutive relations of some tissues of the human head. The results of this project are summarised in this report.

In chapter 2 a literature survey is presented about the constitutive behaviour of skull bone, the cerebral membranes, brain tissue and the cerebrospinal fluid. Attention is paid to the measured variables, the experimental methods and conditions and the constitutive models. A description of the anatomy of the human head is given in appendix A.

Next, a choice is made for the constitutive model to describe the mechanical behaviour of brain tissue (see chapter 3). The experiments, based on this model and the results can be found in chapter 4. A special subject in this chapter is the application of the time/temperature superposition principle, known in polymer science, to obtain material parameters for frequencies relevant for impacts.

In the next chapter fits of the generalised Maxwell model upon the measurements are shown and discussed. The most important conclusions and recommendations are summarised in the last chapter.

2 Literature study to the mechanical properties of brain tissue, dura mater, cerebrospinal fluid and skull bone

In this chapter the mechanical properties of brain tissue, dura mater, cerebrospinal fluid and cranial bone are presented as found in literature. The aim of the study was to make an inventory of the published knowledge of the mechanical properties of the above mentioned materials, together with the experimental methods, used to obtain the data. Further, a survey of the constitutive models, which are based on the experimental results and can used in finite element models to describe the mechanical behaviour of the materials, is put together.

The mechanical properties of the materials are summarised in tables, along with the method to achieve the data. Conclusions about this information can be found in the next section. The sample preparation methods are put together in appendix C.1. In section 2.2 the constitutive relations for the various tissues are discussed. These relations are necessary to describe the mechanical behaviour of the biological structures. The material parameters, as reported in the tables, were used to formulate these relations. Finally, conclusions about the information in the literature are drawn in relation with the aim of this project.

2.1 Reported tissue properties

In table 2.1 the reported mechanical properties of brain tissue are listed. The mechanical properties for dura mater are presented in table 2.2. Investigations for other cerebral membranes were not published. Data on the density and viscosity of cerebrospinal fluid are shown in table 2.3. In table 2.4 the properties are listed for skull bone. It's failure properties are summarised in table 2.5. The information is listed schematic. The physical significance of the reported mechanical properties can be found in many books about Mechanics, for example see Hunter (1983). A very short overview is given in appendix D.

It is difficult to compare the values of the properties that are presented in the various publications. Often information about the experimental method and conditions or sample preparation method is missing or the method is not explained completely. And finally, in some experiments large strains are used which may lead to internal structural damage of the tissues. Investigations to these possible structural changes are not reported. A list is given in appendix C.2 with experimental conditions and other aspects that has to be noted during the experiments. With these gives, it must be possible to compare experimental results. No

publication contains all necessary information.

2.1.1 Linear/Nonlinear behaviour

Galford and McElhaney (1970) showed with the use of creep experiments that brain tissue behaves like a nonlinear viscoelastic material. The tissue does not follow the principle of proportionality (a viscoelastic material is said to show linear behaviour when an increase of the excitation results in a proportional increase of the response). The strains, used in these experiments, lay between 30 and 60%. Therefore, no conclusions can be drawn for small deformations.

Stress-strain plots for dura mater, obtained with uniaxial tensile experiments, were presented by McGarvey et al. (1984). In the plots, a linear relation between stress and strain is observed for strains above 15% and stresses between 0.050–0.2 MPa. The time-dependent behaviour of dura mater was investigated by tensile experiments with different strain rates and creep experiments. The creep compliance satisfies the principle of proportionality, for stresses between 0.52 and 1.55 MPa for human tissue and between 0.60 and 0.97 MPa for Rhesus monkey (Galford and McElhaney, 1970).

Human skull bone shows linear behaviour for both radial (direction perpendicular to skull bone surface) and tangential (direction parallel to skull bone surface) free compression up to a strain of 0.02% (McElhaney et al., 1970). Creep and relaxation experiments were not performed for this material.

The relation between the strain rate and the compressive modulus for bone tissue has only been investigated for the three layers separately. Melvin et al. (1969) compressed samples of diploe layer with strain rates of 0.22 and 2.2 s^{-1} and found no difference for the elastic and failure properties. On the other hand, Wood (1971) showed that for samples, made from the inner or outer table, in tensile experiments the ultimate strength and strain and the elastic modulus varied significantly with the strain rate (see table 2.6). The energy absorbed in a sample till failure did not show any relationship with the strain rate. However, the method to estimate the absorbed energy is unknown. The dependence of the elastic modulus on the strain rate indicates that the tables behave as a viscoelastic material.

2.1.2 Homogeneity/Anisotropy

In their density measurements on brain tissue Barber et al. (1970) did not find any significant differences between gray and white matter and between various locations (except the putamen[11]).

Shuck and Advani (1972) made a comparison between the complex modulus estimated for samples from the corona radiata (purely white matter) and the thalamus (a mixture of white and gray matter). The cylindrical samples were cut in three perpendicular directions. The presented results differ, depending on the origins of the samples and their cut directions but

[1]C = creep experiment; CC = confined compression; DSS, DTS = dynamic simple resp. torsional shear; Ex = pressure measurements during expansion of flexible cylinder in brain; FC = free compression; FV = free vibration; HI = harmonic indentation; In = nonharmonic indentation; TR = transient rotation.

[2]Indentation experiments were performed with skull and dura locally removed, but arachnoid and pia intact.

[3]Same values found for shear modulus with *in vivo* and *post mortem* brains.

[4]Experiments performed by Fallenstein et al. (1969)

[11]putamen = part of the diencephalon

Table 2.1: Experimentally determined mechanical properties of brain tissue

Property	Values/Relations	Method[1]	Reference	Notes
HUMAN				
in vitro				
Density	1.081 ± 0.003 g/cm^3		Barber et al. (1970)	range: 1.001–1.620 g/cm^3
Bulk modulus	2.1 GPa ± 5%	CC	McElhaney et al. (1972)	independent of frequency up to 100 Hz
Creep compliance	$J(t) = 5.15 \cdot 10^{-5} + 3.77 \cdot 10^{-6} \ln t$ Pa^{-1}	C	Galford and McElhaney (1970)	stress range 3.5–6.9 kPa
Complex elastic modulus	$66.7 + j \cdot 26.2$ kPa	FV	Galford and McElhaney (1970)	frequency 34.0 Hz
Shear modulus	1.17–2.19 kPa	TR	Ljung (1975)	prescribed acceleration up to 400000 rad/s^2
Complex shear modulus $G^* = G' + jG''$	G' = 0.6–1.41 kPa G'' = 0.30–0.65 kPa	DSS	Fallenstein et al. (1969)	frequency 10 Hz
	G' = 0.427–0.952 kPa G'' = 0.352–0.600 kPa	DSS	McElhaney et al. (1972)	frequency 10 Hz
	G' = 0.83–138 kPa G'' = 0.3–83 kPa	DTS	Shuck et al. (1970)	frequency 2–400 Hz
	G' = 4.13–10.6 kPa G'' = 1.38–3.51 kPa	DTS	Shuck and Advani (1972)	frequency 2–10 Hz
Kinematic viscosity	0.0014–0.0164 m^2/s	TR	Ljung (1975)	prescribed acceleration up to 400000 rad/s^2
Stress as function of time and strain rate	$\ln \sigma = 0.50 + 0.782 \ln t + \ln \dot{\epsilon}$	FC	McElhaney et al. (1972)	exact strain rates not published
RHESUS MONKEY				
in vitro				
Density	1.100 ± 0.008 g/cm^3		Barber et al. (1970)	range: 1.006–1.444 g/cm^3
Bulk modulus	2.1 GPa ± 5%	CC	McElhaney et al. (1972)	independent of frequency up to 100Hz
Creep compliance	$J(t) = 6.24 \cdot 10^{-5} + 3.76 \cdot 10^{-6} \ln t$ Pa^{-1}	C	Galford and McElhaney (1970)	
Stress as function of time and strain rate	$\ln \sigma = 0.69 + 0.85 \ln t + \ln \dot{\epsilon}$	FC	McElhaney et al. (1969)	exact strain rates not published
Complex elastic modulus	$91.0 + j \cdot 53.8$ kPa	FV	Galford and McElhaney (1970)	frequency 31.0 Hz
in vivo				
Elastic modulus	28–41 kPa	In[2]	Walsh and Schettini (1976)	
	1–60 kPa	Ex	Metz et al. (1970)	
Complex shear modulus $G^* = G' + jG''$	G' = 0.125–0.425 kPa	HI[2]	McElhaney et al. (1972)[3]	frequency 80–100 Hz
	$\overline{G''/G'} = 0.84$	HI[2]	McElhaney et al. (1972)[3]	frequency 80–100 Hz
	$19.5 + j \cdot 11.2$ kPa	HI[2]	Wang and Wineman (1972)[4]	frequency 80 Hz
PIGS				
in vitro				
Dynamic modulus	$\lvert G^* \rvert$ = 0.4–1 kPa	DSS	Bittenberger Arbogast et al. (1995)	frequency 20–100 Hz

Table 2.2: Experimentally determined elastic properties of dura mater

Property	Values/Relations	Method[5]	Reference	Notes
HUMAN				
in vitro				
Density	1.133 ± 0.010 g/cm^3		Barber et al. (1970)	range: 1.050–1.550 g/cm^3
Elastic modulus	41.55 ± 21.63 MPa	T	McElhaney et al. (1972)	strain rate 0.0666 s^{-1}
	44.33 ± 22.32 MPa	T	McElhaney et al. (1972)	strain rate 0.666 s^{-1}
	60.66 ± 25.64 MPa	T	McElhaney et al. (1972)	strain rate 6.66 s^{-1}
Complex elastic modulus	$31.5 + j \cdot 3.4$ MPa	FV	Galford and McElhaney (1970)	frequency 22.0 Hz
Creep compliance	$J(t) = 6.89 \cdot 10^{-8} + 1.41 \cdot 10^{-9} \ln t$ Pa^{-1}	C	Galford and McElhaney (1970)	stress range: 0.517–1.55 MPa
RHESUS MONKEY				
in vitro				
Density	1.189 ± 0.030 g/cm^3		Barber et al. (1970)	range: 1.013–1.569 g/cm^3
Complex elastic modulus	$16.5 + j \cdot 3.3$ MPa	FV	Galford and McElhaney (1970)	frequency 19.0 Hz
Creep compliance	$J(t) = 1.45 \cdot 10^{-9} + 1.84 \cdot 10^{-8} \ln t$ Pa^{-1}	C	Galford and McElhaney (1970)	stress between 0.586–0.965 MPa
BABOON				
in vitro				
Elastic modulus	35–140 MPa	I	Margulies (1987)	
MONGREL DOG				
in vitro				
Elastic modulus	0.399 MPa	T	Tunturi (1977)	weights between 200–300 N
	46.3 MPa	T	Tunturi (1977)	weights between 500–1500 N
in vivo				
Elastic modulus	22 MPa	WPP	Liu et al. (1976)	frequency 40–300 Hz
	3.6 MPa	WPA	Liu et al. (1976)	frequency 40–300 Hz
Shear modulus	0.18 MPa	WPT	Liu et al. (1976)	frequency 40–180 Hz

[5]C = creep; FV = free vibration; I = Inflation; T = Tension; WPA, WPP, WPT = wave propagation with axial, pressure and torsional waves, respectively.

Table 2.3: Experimentally determined mechanical properties for cerebrospinal fluid

Property	Values	Reference	Notes
HUMAN			
in vitro			
Density	1.007 ± 0.008 g/cm^3	Barber et al. (1970)	range: 0.958–1.163 g/cm^3
Density	1.006–1.008 g/cm^3	Duck (1990)	
Relative viscosity	1.020–1.027	Ommaya (1968)	water: 1.000

Table 2.4: Experimentally determined elastic properties of cranial bone.

Property	Values/Relations	Method[6]	Reference	Notes
HUMAN				
in vitro				
Thickness	6.91 ± 1.19 mm		McElhaney et al. (1970)	
Density	1.41 ± 0.53 g/cm^3		McElhaney et al. (1970)	
Elastic modulus	0.4–2.8 GPa	RC	Melvin et al. (1969)	
	2.4 ± 1.5 GPa	RC	McElhaney et al. (1970)	
	5.6 ± 3.0 GPa	TC	McElhaney et al. (1970)	
	7.8–15.3 GPa	B3	Hubbard (1971)	
Shear modulus	150–750 MPa	B3	Hubbard (1971)	
Poisson's ratio	0.19 ± 0.08	RC	McElhaney et al. (1970)	
	0.22 ± 0.11	TC	McElhaney et al. (1970)	
Relation between elastic modulus and density	$E_R = 2.27 \cdot 10^{-7} \cdot \gamma^{5.13}$ Pa	RC	Melvin et al. (1969)	C[7] = 0.86
	$E_R = 9.0\gamma - 9.0 \cdot 10^3$ MPa	RC	McElhaney et al. (1970)	C = 0.62
	$E_T = 11.5\gamma - 10.5 \cdot 10^3$ MPa	TC	McElhaney et al. (1970)	C = 0.65
Diploe layer separately				
Thickness	2.74 ± 1.07 mm		McElhaney et al. (1970)	
Shear modulus	14 ± 10 MPa	To	McElhaney et al. (1970)	
	110–550 MPa	B3	Hubbard (1971)	
MONKEY				
in vitro				
Thickness	2.57 ± 0.25 mm		McElhaney et al. (1970)	
Density	1.80 ± 0.28 g/cm^3		McElhaney et al. (1970)	
Elastic modulus	6.5 ± 3.2 GPa	TC	McElhaney et al. (1970)	

[6]B3 = three-point bending (quasi-static); RC, TC = radial resp. tangential compression (v = 0.25 mm/s); To = Torsion

[7]C = correlation coefficient

information about sample dimensions and spread of data were not given. Therefore, further conclusions cannot be drawn.

Bittenbender Arbogast et al. (1995) performed simple shear relaxation experiments with samples, originating from the pons. In this part of the central nervous system the fibres are supposed to be organised mainly in longitudinal direction but this assumption is not accompanied by a histological investigation of the samples. The directional dependence was examined mechanically by shearing the same sample both parallel and transverse to the assumed predominant direction of the axonal fibres. The data suggest anisotropic behaviour (more evident at large strains). Biological variation, however, prevents statistical analysis.

(Barber et al., 1970) estimated the density for dura mater samples from several locations. No significant differences were found. Uniaxial tensile experiments with different strain rates did not give any statistical evidence for anisotropic behaviour (see for example McElhaney et al. (1972)), as can be expected from the thoroughly interwoven structure of the tissue (see appendix A).

No difference was found in the elastic or failure properties between samples from the inner table and the outer table 1) from the same bone type and 2) from different bone types (parietal, frontal and occipital bone) by Wood (1971).

The elastic modulus in radial direction for samples of skull bone from different locations

Table 2.5: Ultimate strength and strain for cranial bone (estimated *in vitro*).

Property	Values/Relations	Experiment[8]	Reference	Notes
HUMAN				
Ultimate strength	73.8 ± 35 MPa	RC	McElhaney et al. (1970)	
	97 ± 36 MPa	TC	McElhaney et al. (1970)	
Ultimate strength				
diploe layer	21 ± 3 MPa	S	McElhaney et al. (1970)	
	12.5–78.2 MPa	RC	Melvin et al. (1969)	
	22 ± 6 MPa	To	McElhaney et al. (1970)	
Ultimate strain	$0.097 \pm 0.080\%$	RC	McElhaney et al. (1970)	
	$0.051 \pm 0.032\%$	TC	McElhaney et al. (1970)	
Ultimate strain				
inner and outer tables	$0.51 \pm 0.16\%$	B3	Hubbard (1971)	
	$0.52 \pm 0.12\%$	Te	Hubbard (1971)	
Relation ultimate radial strength				
with density[9]	$\sigma_{RU} = 1.8 \cdot 10^{-3}\gamma^{3.3}$ Pa		McElhaney et al. (1970)	$C = 0.91$
Relation ultimate tangential strength				
with density[10]	$\sigma_{TU} = 0.19\gamma - 1.8 \cdot 10^{2}$ MPa		McElhaney et al. (1970)	$C = 0.65$
MONKEY				
Ultimate strength	92.4 ± 50 MPa	To	McElhaney et al. (1970)	
GOAT				
Ultimate strength	259 ± 4.3 MPa	B3	Jaslow (1990)	

[8] B3 = three-point bending (quasi-static); RC, TC = radial resp. tangential compression (v = 0.25 mm/s); S = Shear; Te = Tension; To = Torsion.
[9] σ_{RU} = ultimate radial strength.
[10] σ_{TU} = ultimate tangential strength.

of the parietal, occipital and frontal bones displays significant variations (McElhaney et al., 1972). These variations are related to the density of the samples (see table 2.4). Linear regression of the ultimate strength versus the elastic modulus (in compression) in radial and tangential direction yields correlation coefficients of 0.78 and 0.57, respectively. For samples containing all three layers, no anisotropic behaviour was determinated with simple shear experiments in tangential direction.

2.1.3 Degeneration

In this section two subjects are discussed, the differences between *in vivo* and *post mortem* properties and the *in vitro* properties as function of time after sacrifice of the donor.

With indentation experiments Metz et al. (1970) found a decrease of the elastic modulus of 50% within 45 minutes after the donor was sacrificed. McElhaney et al. (1972) found little (not quantified) differences between the results of indentation experiments under *in vivo* and *post mortem* conditions. These experiments produced complex moduli that were approximately twice those given by the *in vitro* shear experiments. The authors related this difference only to the geometry of the probe tip used as the indentor and not to the different frequency ranges (10 Hz for the *in vitro* experiments and 80–100 Hz for the *in vivo* experiments, see table 2.1). They concluded that the flat-plate shearing properties were valid indicators for the complex modulus of human brain tissue under *in situ* conditions but this is disputable. When *in vivo* and *post mortem* properties of brain tissue are compared, influences of, for example the blood pressure, have to be eliminated. The above mentioned publications do not contain

Table 2.6: Linear regression of failure properties against the logarithm of strain rate for $0.005 \leq \dot{\epsilon} \leq 150$ s^{-1} estimated in tension with samples from the inner and outer tables, (Wood, 1971)

	Elastic modulus vs. $^{10}\log \dot{\epsilon}$	Ultimate strength vs. $^{10}\log \dot{\epsilon}$	Ultimate strain vs. $^{10}\log \dot{\epsilon}$	Absorbed energy vs. $^{10}\log \dot{\epsilon}$
Intercept	16.0 GPa	82.7 MPa	0.63%	294 kJ
Slope	1.9 GPa/decade	6.9 MPa/decade	-0.04 %/decade	-1.4 kJ/decade
Standard deviation for slope	69 MPa/decade	1.2 MPa/decade	0.01%/decade	0.9 kJ/decade

investigations to these influences.

Immediately after the sacrifice of the donor, degeneration processes will start. Enzymes will break down proteins and cell walls. Probably the constitutive behaviour of brain tissue will be altered, because it's structure is changed. It is suggested that the most important part of this degeneration process happens in the first hour after the sacrifice (McIlwain, 1966). However, an extensive description of the degeneration of brain tissue after the sacrifice of a donor is not available yet. McElhaney et al. (1972) reported that no significant changes were found in the mechanical properties of brain tissue, dura mater and skull bone determined under *in vitro* conditions over a period of 15 hours. However, these observations can only be considered as an indication (see the introduction of section 2.1).

2.1.4 Comparison between human and animal tissue properties

A comparison between the experimental results with human and animal brain tissue and dura mater cannot be made. First, experimental conditions (like elapsed time after death of the donor) are often unknown. Secondly, the origin and composition of the samples are not described and thirdly, the experimental methods are not comparable.

Very little information has been found about the mechanical behaviour of animal cranial bone, so comparison between human and animal cranial bone cannot be made. More information about the simularities and differences between bone tissue of animals and humans can be found in publications about other bone tissues.

2.1.5 Influence of age of the donor

The influence of the age upon the mechanical properties of human dura mater was investigated on donors in the fetal stage. Bylski et al. (1986) did not find any statistical evidence in contrast with Kriewall et al. (1983). The results could not be compared with the results of human adult dura mater, given in table 2.2, because different material properties were estimated under incommensurable conditions.

Wood (1971) investigated the influence of age upon the tensile elastic modulus of skull bone. He estimated that this modulus was higher for samples from young donors than for old people. The difference was about 7% at a strain rate of 1 s^{-1}. Jaslow (1990) did not find any significant difference in the elastic and failure properties of skull bone beams of young and old female goats in three point bending experiments.

2.1.6 Influence of sutures on the behaviour of skull bone

Beamshaped skull bone samples with a suture in the midregion were used in bending experiments by Hubbard et al. (1971) and the results were compared with the response calculated with a model, used to describe the experiments with samples without a suture. The comparison indicated that these samples were about 50% more compliant to flexure about an axis along the sutures than samples with an equal beam geometry but without a suture.

Four-point bending experiments were performed with beam shaped samples to investigate the influence of a suture on the strength. Samples with sutures were less strong than the adjacent cranial bone for quasi-static bending. A quantification was not given (Hubbard et al., 1971).

2.2 Constitutive relations

Brain tissue

Both linear and nonlinear viscoelastic models were fitted upon the creep experiments of Galford and McElhaney (1970), the compression experiments of Estes and McElhaney (1970) and the shear experiments of Shuck and Advani (1972). The presented fits of a linear viscoelastic model for fluids (the Burgers model, explained in Findley et al. (1976)) could not be verified, the calculations showed completely different results from those published. The Burgers model with a nonlinear quadratic dashpot and spring and a Mooney-Rivlin (MR) model, modified to be used for viscoelastic materials, were also used to describe the behaviour of brain tissue (Pamidi and Advani, 1978), (Mendis, 1992). The use of the MR model is interesting because this model can be used to describe the constitutive behaviour of a solid under large deformations. Time dependent behaviour was included in the parameters of the model or included by using dissipation. Due to the reasons, noted in the introduction of section 2.1, conclusions about the use of the models cannot be made.

Bittenbender Arbogast et al. (1995) used a quasi-linear viscoelastic theory to model the stress relaxation tests. The model is characterised by an instantaneous elastic function (a polynomial) and a reduced relaxation function (generalised Maxwell model for solids, see section 3.2 for a description). The fitted relaxation times were not dependent of the direction of the fibres in contrast with the spring rigidities. The instantaneous elasticity differed for the two used shear directions but due to the large biological variations no conclusions could be made about the value of the fitted parameters in relation to the shear direction.

Dura mater

Biaxial tensional experiments were performed by clamping circular samples of dura mater, inducing a pressure difference between inner and outer sides and measuring the apex deflection. These measurements were modelled by Kriewall et al. (1983) and Bylski et al. (1986) using both the Mooney-Rivlin (MR) and the Skalak, Tozeren, Zarda and Chien (STZC) nonlinear elastic models. Both publications showed that the SZTC model yields a better fit to the experimental results than the MR model. The best fit of the MR model diverges from the membrane responses at large apex deflections, in contrary to the SZTC-model. Time-dependent behaviour is not included although dura mater is viscoelastic (see section 2.1.1).

Skull bone

A phenomenological model was derived by McElhaney et al. (1970), called "porous block model". It was assumed that skull bone can be regarded as a skeleton of cranial bone, consisting of blocks of compact bone (elastic modulus equal to 12 GPa). The voids in the diploe layer were represented by omitting blocks. The tangential distribution of these voids was homogeneous and the radial distribution was estimated to be Gaussian. Finally, it is assumed that local mechanical responses are proportional to the local density raised to some power (γ^n). It was found that maximum correlation with the measurements was obtained with the power n equal to 3 (C= 0.79). Fitting the same model for the ultimate strength, the best fit (C = 0.67) occured when the power n was equal to 4, taking 0.14 GPa for the ultimate strength of compact bone.

Three-point bending experiments (Hubbard, 1971) were used to validate a linear layered beam theory (Plantema, 1965). The beam samples were considered in this theory as a three-layered beam (two compact bone layers separated by a less stiff layer) and it was assumed that the shear modulus for the diploe layer was half the elastic modulus for the tables (equal to 11.8 GPa, compact bone). The values for the global shear and elastic modulus, estimated with this theory, compared well with the results from calculations based upon a simple beam theory.

2.3 General conclusions

The experimental determination of the mechanical properties of brain tissue and cerebral membranes is still in a beginning stage. The values in table 2.1 and 2.2 can only be used as indications. The discussed aspects in section 2.1 are mostly incompletely examined. The reported values, however, for various material parameters of brain tissue do overlap (complex shear modulus, elastic modulus). For dura mater, no material parameters were reported, obtained with different experimental methods.

The most interesting constitutive model, used to describe the behaviour of brain tissue is the Mooney-Rivlin model because it is a model for solids. However, this model is only used to describe incompletely reported results. The SZTC-model, used to describe the behaviour of dura mater, does not include time-dependent behaviour. No investigation has been carried out to physical or geometrical (non-)linearities. Further, reliable data for the constitutive behaviour of brain tissue and cerebral membranes in frequencies, relevant for impacts is not found. This implicates that with the published information a well-founded choice for a constitutive model for brain tissue or dura mater cannot be made.

The material parameters for skull bone are extensively reported for quasi-static deformations. Each parameter is mostly only in one publication reported except the elastic and shear modulus. The values estimated with the three-point bending experiments do not correspond with the values estimated with other experimental methods. The use of the layered beam theory and the porous block model to describe the bone tissue as a linear elastic material produced interesting results. If the thicknesses of the tables and the diploe layer are measured for the whole skull (for example with Computer Tomography) it could be possible to estimate the local elastic moduli using this theory. Models that incorporate the time-dependent behaviour of skull bone, as presented in table 2.6, are not used, so constitutive relations for skull bone to describe the behaviour in impacts are still not found.

3 The constitutive model

3.1 Assumptions for constitutive behaviour of brain tissue

From the experimental results, published in literature, it is concluded that brain tissue is viscoelastic. However, it is not possible to select a constitutive model on the basis of the conclusions of the literature study (see section 2.3). For pragmatic reasons, some simplifying assumptions are made about the mechanical behaviour of brain tissue.

First, it is commonly known that biological tissues display mostly physically nonlinear behaviour. Results presented in section 2.1.1 indicate that brain tissue is not an exception to this rule. However, to simplify the project, the behaviour is considered to be physically linear. Next, brain tissue is considered in this report as an isotropic material, although in some parts of the central nervous system, like the *corpus callosum* and the spinal cord, the fibres are assumed to be organised in one direction. Further, brain tissue will be described as a solid because it's consistency prevents a description as a liquid (Dodgson, 1962). Fourth, the literature study did not yield any reliable descriptions of the behaviour of brain tissue in either geometrically linear or nonlinear conditions. Therefore, as a start, only geometrically linear conditions are used. Large deformations which are likely in impacts, will be investigated when the behaviour of brain tissue in linear geometric situations is understood. Finally, the material behaviour will be only considered in a one-dimensional situation.

With these five assumptions (geometrical and physical linearities, isotropy, solid, one-dimension) a one-dimensional linear viscoelastic model could be used to describe the constitutive behaviour. In appendix B a short explanation is given about the parameters used to describe the between stress and strain for a one-dimensional linear viscoelastic material. A usefull constitutive model for brain tissue is the generalised Maxwell model. A description for this model is given in the next section.

The use of a linear viscoelastic model generates an advantage to find solutions for the time dependent reponse for a linear viscoelastic material in some stress situations. The time variable in the problem can be removed by employing the Laplace transformation when two conditions are satisfied: the temperature has to be constant and the interface between the surface(s) on which the stress is prescribed and the surface(s) on which the displacements are described, has to be independent of time. However, the conditions prescribed on these surfaces themselves can be time-dependent. The problem is thus converted to an equivalent elastic problem. When a solution of the problem has been found, the inverse Laplace transformation yields the solution in time variable t for the time dependent behavior. The method is called the "correspondence principle". More information about the criteria to use this principle together with examples are given by Findley et al. (1976).

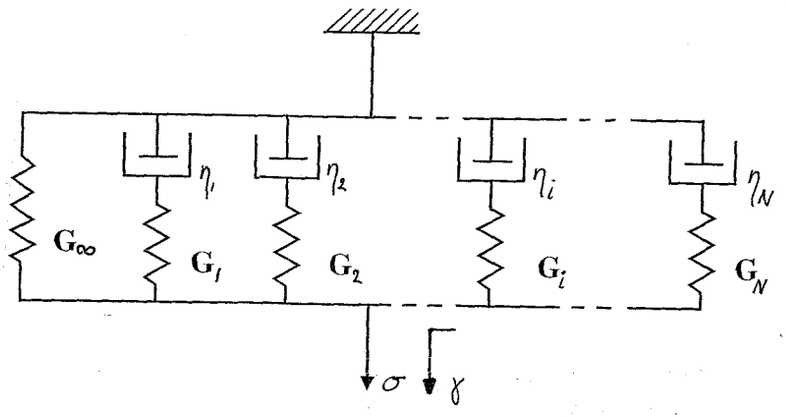

Figure 3.1: Schematic view of the generalised Maxwell model

3.2 Generalised Maxwell model for solids

A generalised Maxwell model consists of a parallel arrangement of N Maxwell elements and one spring. Each Maxwell element is composed of a dashpot and a spring in series (see fig. 3.1). In this model a spring stiffness and a damping constant are identified with a shear modulus G and viscosity η. Force and strain are replaced by stress σ and strain γ respectively. The relation between stress and strain for the Maxwell element with index i ($i = 1, 2, ..., N$) is:

$$\dot{\gamma}(t) = \frac{\dot{\sigma}_i}{G_i} + \frac{\sigma_i}{\eta_i} \tag{3.1}$$

The ratio η_i/G_i is defined as the relaxation time τ_i.
For a relaxation experiment the solution for the stress as function of time is given by:

$$\sigma_i(t) = \gamma_0 G_i e^{-\frac{t}{\tau_i}} \tag{3.2}$$

The term $G_i e^{-\frac{t}{\tau_i}}$ is the representation by one Maxwell element for the relaxation modulus $G(t)$. To obtain a relation between stress and strain for the frequency domain instead of the time domain, a Fourier transformation must be applied upon (3.1). The complex modulus, defined in appendix D, for one Maxwell element is given by:

$$G'(\omega) = G_i \frac{\omega^2 \tau_i^2}{1 + \omega^2 \tau_i^2} \tag{3.3}$$

$$G''(\omega) = G_i \frac{\omega \tau_i}{1 + \omega^2 \tau_i^2} \tag{3.4}$$

To obtain the relation between stress and strain for a system that consists of N Maxwell elements, first, relation (3.1) is rewritten according to Findley et al. (1976) as:

$$\sigma_i = \left[\frac{D}{\frac{1}{\eta_i} + \frac{D}{G_i}} \right] \gamma \tag{3.5}$$

where D is the differential operator with respect to time $D = \frac{d}{dt}$. The sum of the stresses of each Maxwell element is equal to the total stress upon this system:

$$\sigma = \sum_{i=0}^{N} \sigma_i(t) = \left[G_\infty + \sum_{i=0}^{N} \frac{D}{\frac{1}{\eta_i} + \frac{D}{G_i}} \right] \gamma \tag{3.6}$$

The extra spring, added to describe a solid, is represented by G_∞. The relaxation times together form the relaxation spectrum. Equation (3.6) can be rewritten by:

$$\sum_{k=0}^{N} p_k \frac{d^k}{dt^k} \sigma = \sum_{l=0}^{N} q_l \frac{d^l}{dt^l} \gamma \tag{3.7}$$

The material parameters p_i and q_i can be determined by (3.6).
With this model the stress as function of time in a relaxation experiment is given by:

$$\sigma(t) = \gamma_0 \left[G_\infty + \sum_{i=1}^{N} G_i e^{-\frac{t}{\tau_i}} \right] = \gamma_0 G(t) \tag{3.8}$$

The storage and loss modulus for N Maxwell elements are represented by:

$$G'(\omega) = G_\infty + \sum_{i=1}^{N} G_i \frac{\omega^2 \tau_i^2}{1 + \omega^2 \tau_i^2} \tag{3.9}$$

$$G''(\omega) = \sum_{i=1}^{N} G_i \frac{\omega \tau_i}{1 + \omega^2 \tau_i^2} \tag{3.10}$$

With both relaxation and dynamical experiments the model parameters τ_i and G_i can be estimated. Parameters, estimated by relaxation experiments, can be used to describe the results obtained with dynamical experiments. This is a method to compare the results of both kinds of experiments.

4 Shear Experiments on brain tissue

In this chapter the experiments to examine the constitutive behaviour of brain tissue that are performed in this project, are described. In section 4.1 the experimental setup to investigate the frequency dependent behaviour of the viscoelastic properties will be presented. The experimental results are discussed in section 4.2. A special subject of this chapter is the application of the time/temperature superposition principle to brain tissue to obtain the material properties at frequencies relevant for impacts. In the last section the conclusions, drawn from the shear experiments are presented.

4.1 Experimental setup

Tensile experiments, which are commonly used to investigate the constitutive behaviour of solids, are difficult to perform with brain tissue, because clamping is difficult. Confined compression experiments are not useful because brain tissue is nearly incompressible (see table 2.1). Secondly, deformations in the human head under confined compression conditions are not likely, because the human skull has gaps, like the eye sockets. Unconfined compression experiments with brain tissue are difficult to perform and to analyse, for example because the deformation is two-dimensional.

Shear experiments are a common method to characterise viscous fluids (see for example Macosko (1994)) but can also be used to investigate the behaviour of soft solid tissues as brain tissue. Further, Holbourn (1943) indicated that brain tissue is highly susceptible to high levels of shear strain due to its incompressibility and lack of rigidity. When the human head suffers fast rotations, it is assumed that brain tissue undergoes large shear strains. Fast rotation experiments with physical models justified these assumptions (Margulies, 1987). The shear properties of brain tissue are needed before models can be developed that describe these experiments. So, shear experiments are an appropriate method to investigate the constitutive behaviour of brain tissue. These experiments were performed with a rheometer which is capable to perform torsional shear experiments on liquids and soft tissues, the Rheometrics Fluids Spectrometer II (RFS II).

Cylindrical samples with a height of 1–2 mm, a diameter of 10–12 mm and flat upper and lower sides were prepared from calf brains. On the RFS II they were sheared between two flat plates. The preparation method for the samples is described in appendix C.3. With the plate-plate configuration relaxation and dynamical shear experiments were carried out. During these experiments the temperature was 37°C and a moist chamber was used to prevent dehydration of the sample.

A schematic view for the plate-plate configuration can be found in fig. 4.1. The sample

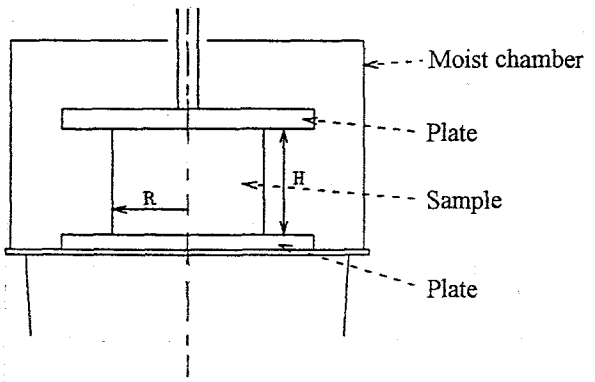

Figure 4.1: Schematic view of the RFS II (not on scale)

(with radius R and height H) is centred between the flat plates. The lower plate enforces an angular displacement upon the sample. The induced moment on the standstill upper plate is measured. To evaluate the viscoelastic properties it is assumed that the sample sticks to both plates. The distance between both plates does not change during the experiments. Further, inertial effects are neglected. With these assumptions, the angular displacement of a plane of the cylindrical sample at distance z to the lower plate can be described by:

$$\phi(z,t) = \alpha(t)\frac{H-z}{H} \tag{4.1}$$

where $\alpha(t)$ is the angular displacement of the lower plate (in radians). A schematic view of the directions of the enforced displacement by the lower plate on the sample and the torque upon the upper plate together with the variables $\alpha(t)$, $\phi(t)$ and z can be found in fig. 4.2. The shear strain is defined as:

$$\gamma(t) = -R\frac{\partial}{\partial z}\phi(z,t) = R\frac{\alpha(t)}{H} \tag{4.2}$$

To obtain a geometrically linear deformation, as assumed above, the deformations and the gradients of the deformations have to be small (Koiter, 1985). In this load case, this corresponds to $\sin\alpha(t) \approx \alpha(t)$ and $R\frac{\partial\phi}{\partial z} \gg \left(R\frac{\partial\phi}{\partial z}\right)^2$. Calculations showed that these conditions were satisfied for all load cases used in this report (see appendix D).

For relaxation experiments, the enforced angular displacement at the lower plate ($z = 0$) is equal to zero for $t < 0$ and equal to α_0 for $t \geq 0$. The relaxation modulus $G(t)$ is related to the measured torque $M(t)$ by:

$$G(t) = \frac{2HM(t)}{\pi R^4 \alpha_0} \tag{4.3}$$

For the dynamic shear experiments the lower plate oscillates around the axis of symmetry (shown in fig. 4.1) with an angle amplitude α_0 and an angular frequency ω:

$$\alpha(t) = \mathrm{Re}(\alpha_0 \exp(i\omega t)) \tag{4.4}$$

To define the strain in dynamic experiments, the amplitude α_0 is used, the time-dependent exponent is neglected. Because it is assumed that the material between the plates is linear

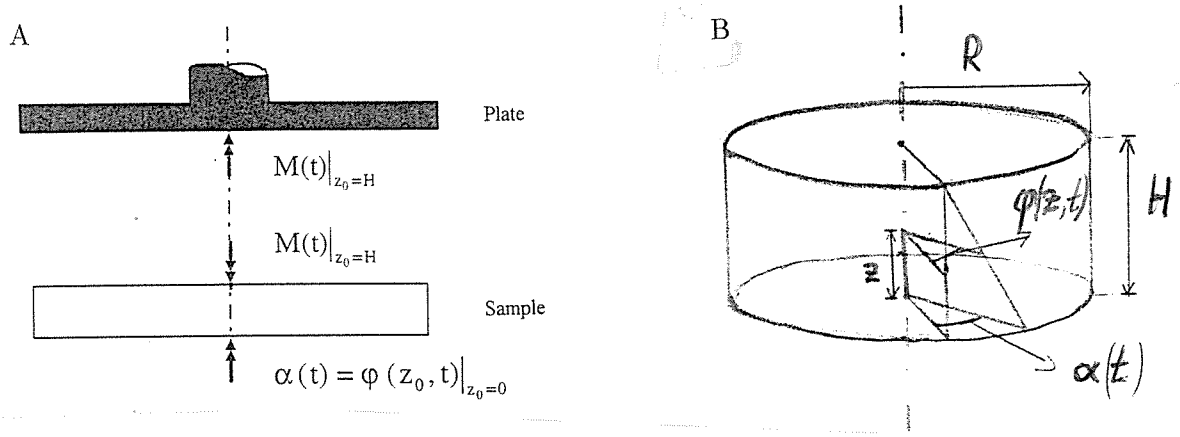

Figure 4.2: (A) Schematic view of the direction of the torque on the upper plate, induced by the enforced displacement of the lower plate. (B) Schematic view of $\alpha(t)$, $\phi(t)$ and z.

viscoelastic, the torque on the upper plate should have the same angular frequency as the enforced displacement:

$$M(t) = \mathrm{Re}(M_H \exp(i\omega t + \delta)) \tag{4.5}$$

where M_H is the amplitude of the measured torque and δ is the phase angle between the measured torque and the enforced displacement. During the experiments an oscilloscope is used to check the shape of the curves for the enforced angular displacement and the measured torque. If slip or another nonlinear event occurs the shape of the torque curve is not sinusoidal. Under geometrically linear conditions the storage modulus and loss modulus (resp. G', G'') are related to the measured quantities M_H and δ by:

$$G'(\omega) = \frac{2HM_H}{\pi R^4 \alpha_0} \cos\delta(\omega) \tag{4.6}$$

$$G''(\omega) = \frac{2HM_H}{\pi R^4 \alpha_0} \sin\delta(\omega) \tag{4.7}$$

The dynamic modulus and the loss angle are defined in appendix D. A concise description of the derivation of the above equations can be found in (Whorlow, 1992).

As stated in section 3.1, the generalised Maxwell model (with the spring moduli and the relaxation times as material parameters) for solids is used to describe the constitutive behaviour of brain tissue in these experiments. The performed relaxation experiments lasted for about 300 s. The sampling rate was about 1 Hz. Relaxation times (see section 3.2), that can be examined with these experiments, are much larger than 10 s. The dynamic experiments are performed with frequencies between 0.0159–15.9 Hz. The maximal frequency is limited by inertial effects in the RFS II and cannot be changed. Roughly, the relevant relaxation times, necessary to describe these measurements, are in the range 0.06–6 s (reciprocal values of the frequency range).

4.2 Results

As said at the end of section 4.1 dynamic experiments do give a better representation of impact conditions than relaxation experiments. Therefore, dynamic experiments are performed with

brain tissue and some results are presented in this section. First, the assumption to consider the mechanical behaviour of brain tissue as physical linear will be investigated. Secondly, the reproducibility of the measurements is discussed in section 4.2.2. Finally, other aspects are discussed in the last subsection.

4.2.1 Physically linear behaviour

To simplify the analysis of the measurements, the brain tissue was assumed to behave linear viscoelastic. This assumption was verified by two different methods. First, an oscilloscope was used to compare visually the enforced angular displacement and the measured torque during the experiments. The images of both curves were sinusoidal with equal frequency. This is an indication that only a phase difference existed between those curves. Further, experiments were carried out with constant frequency but increasing strain amplitude. A typical result is shown in fig. 4.3 (sample data see appendix E). The strain is varied between 0.2 and 2% at a frequency of 15.9 Hz. The dynamic modulus and the loss angle are calculated by (4.6), (4.7) together with (B.12) and (B.18). The relation between the enforced strain and first the dynamic modulus and secondly the loss angle is statistically investigated for strains up to 1%. Both parameters do not correlate significantly with the enforced strain at the 5% level using a student's t-test (see for example Chatfield (1989)). In section 4.1 the deformation is considered as geometrically linear. Thus, the behaviour of brain tissue for shear strain between 0.2–1% can be considered as physically linear with an uncertainty of 5%. When strains larger than 1% are included, a significant correlation is found between the dynamic modulus and the enforced strain.

4.2.2 Reproducibility

In fig. 4.4 a typical result is shown for the dynamic shear experiments. A sample, origin see appendix E, is sheared with frequencies between 0.159 and 15.9 Hz with a 1% strain.

An important method to investigate the reliability of the measurements is to consider the reproducibility i.e. to compare with each other the results of two identical experiments, performed consecutively with the same sample under equal conditions. This comparison is carried out with the Wilcoxon's signed rank test (see (Sokal and Rohlf, 1981)). The difference between the experiments, presented in fig. 4.4, is significant at the 1% level. Thus the measurements on this sample, with $\Delta t = 5$ min, are not reproducible. This result is typical for all measurements performed with brain tissue.

4.2.3 Discussion

Various aspects that influence the measurements and calculations are discussed in this section.

The distance between the upper and lower plate is adjusted by measuring the normal force upon the upper plate (see appendix C.3). When the upper and lower surface of the cylindrical samples are not parallel or not flat, the final adjustment can be reached although not the whole upper surface of the sample sticks to the upper plate. These variations induce an uncertainty on the adjustment of the distance of 50 μm (about 5%).

Large errors are introduced in the computation of the storage and loss moduli with equations (4.6) and (4.7) caused by the measurement of the radius of the sample, by deviations from the assumed circular shape of the sample and by bad alignment of the centre of the sample with the axis of symmetry of the RFS II.

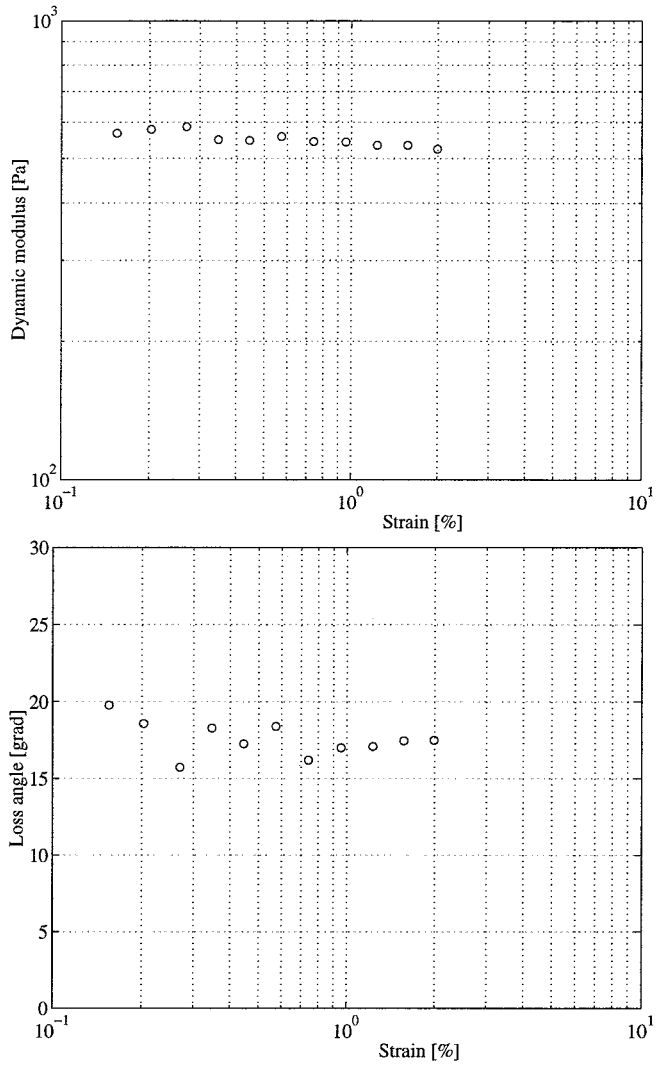

Figure 4.3: Dynamic modulus and loss angle for strain amplitudes in the range 0.2–2.0% demonstrating physically linear behaviour of brain tissue sample (see appendix E) at 15.9 Hz.

The diameter of a sample, placed upon the lower plate of the RFS II, is measured with an accuracy of about 0.5 mm. For a sample with a radius of 6 mm, this can introduce an error of 15% in the calculation of the dynamic modulus.

A sample can be placed eccentric upon the lower plate. For a sample with a radius of 5.5 mm and a distance of 0.5 mm between axis of symmetry and the axis of symmetry of the RFS II, the measured torque is about 1% larger than for the same sample placed concentric on the lower plate.

If the contour of the sample is not exactly circular but elliptic, another error is made. An indication of this error is obtained by comparing the results for a circular sample with radius $R = 5.75$ mm with that of an elliptic sample with principal lengths $a = 6.0$ mm and $b = 5.5$ mm. With these dimensions both samples have an comparable surface area. Further both samples have equal material properties. The equations, given in section 4.1 to calculate the material properties with the measured torque and loss angle, are not valid for the elliptic samples. The different shape results in different relations between the measured torque and the material parameters. For the elliptic sample, the measured torque will be about 10%

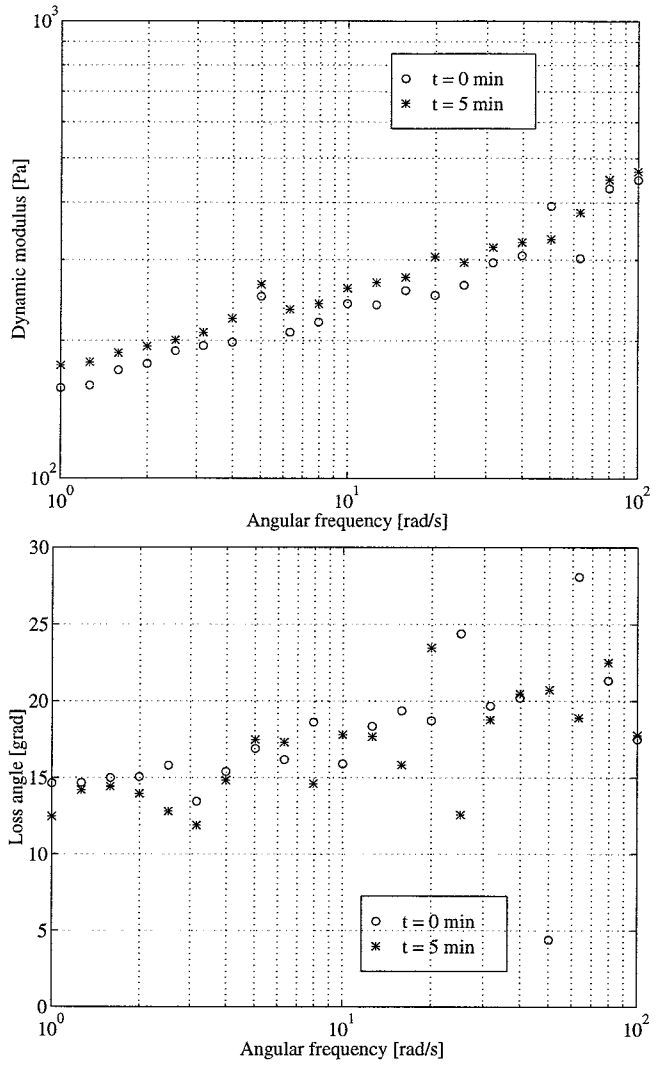

Figure 4.4: Dynamic modulus and loss angle as function of the enforced frequency. The enforced strain is 1%. The sample data can be found in appendix E

higher than the torque, obtained with a circular sample due to the different shape.

The minimal torque, the RFS II is capable to measure, is $2 \cdot 10^{-7}$ Nm. The measured torques were in the range $4 \cdot 10^{-7}$ to $6 \cdot 10^{-6}$ Nm. This indicates that the measurement errors can be quite large (up to 50%).

About sixty samples were used in the torsional shear experiments. The dynamic shear moduli, obtained with the dynamic experiments, were in the range of 65–300 Pa at 0.159 Hz and 300–1000 Hz at 15.9 Hz. These variations could not be related to the origin or orientation of the samples in the animal brain although a systematic investigation to these relations is not performed.

In addition to the measurement error, related to the measurement of the torque and the calculation of the moduli, other aspects can be responsible for these variations like blood vessels. Their shear and elastic moduli are much larger than the shear moduli presented in this report for brain tissue. However, no investigation has been carried out to estimate their influence. The results can be influenced by the preparation method, too. Structural changes can be induced by using the rotating hollow bore or the envelopment by the gelatine.

Again, no investigation has been performed to get an indication of the influence upon the internal structure of the samples. It must be noticed that for all samples the preparation and the experiments were performed under conditions, that were the same as much as possible. Finally, a predominant direction of the fibres can introduce anisotropic behaviour. In that case, samples with different origin and orientation will have different material properties. This aspect can only be investigated by an histological examination of the sample, which is not performed in this project.

4.3 Time/temperature superposition principle

The frequency range of the RFS II is 0.159–15.9 Hz. A range for the typical time duration of the loads in traffic accidents is 1–50 ms (Wismans et al., 1994). Roughly, this range corresponds to a frequency range of 20–1000 Hz. This range does not correspond to the frequency range of the RFS II. A method to estimate the material properties in the relevant frequency range is found in polymer science.

Brain tissue consists of polymers like proteins and lipids (see table A.1). To characterise the rheologic properties of linear viscoelastic polymers for a wide frequency range (wider than the limited frequency range used in the measurements), the time/temperature superposition principle is often used. In literature, no publication is found that contains a description of the application of this principle upon a biological tissue. In this section, the results of the investigation to the application of this principle on brain tissue are presented. First, an explanation of the time/temperature superposition principle or method of reduced variables (in this report also referred to as "the principle") is given. Then criteria, a material has to satisfy before the principle can be applied, are presented using the generalised Maxwell model for solids. In polymer science the principle is applied to materials consisting of only one component. Brain tissue is a composition of many polymers and therefore an extra criterium will be added (see section 4.3.3). Further, some important experimental aspects will be discussed. Finally, the results of the application of the principle will be presented and discussed.

4.3.1 Brief explanation of the basis of the principle

In polymer science it is noticed that viscoelastic characteristics (for example the dynamic modulus as a function of ω) are dependent on the temperature at which the characteristics are measured. Visual inspection of a set isothermal characteristics, obtained at equal time or frequency range but at different temperatures, indicated that these characteristics can be shifted along the logarithmic frequency or time axis to form one smooth curve. The characteristics are shifted to an arbitrarily chosen characteristic of this set and this curve is called the "master curve". The corresponding temperature of the chosen characteristic is referred to as the reference temperature T_0. When the reference temperature is chosen, the shift only depends on the difference between the reference temperature and the temperature of the shifted characteristic. The constructed master curve covers several decades of the time or frequency range while the separate experiments are performed on a smaller time or frequency range. Besides the horizontal shift, also a small vertical shift of the curves has to be applied. This shift is assumed to correspond to variations in the density of the investigated material as a function of the temperature.

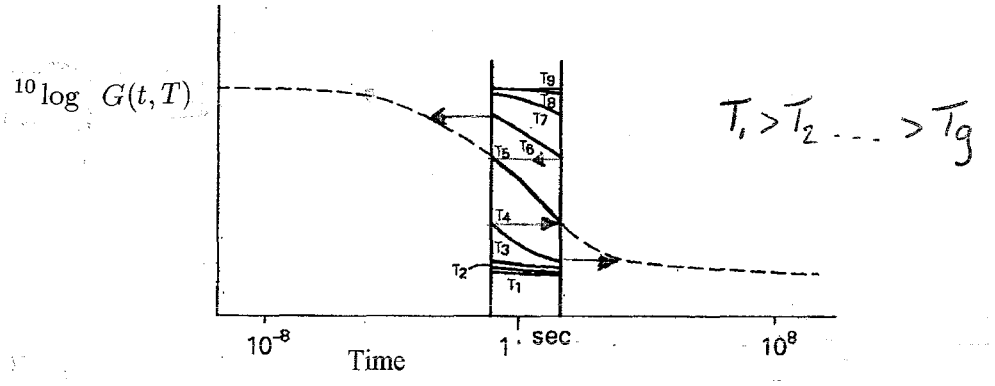

Figure 4.5: Example of a set isothermal characteristics together with the master curve for the relaxation modulus as a function of time (Van der Vegt, 1992). For two characteristics the shifts are denoted.

In fig. 4.5 an example is shown of a relaxation modulus, measured on a limited time range at 9 different temperatures. The characteristic, measured at temperature T_5, is chosen to be the master curve. The other characteristics are horizontally shifted until one smooth master curve is constructed. Characteristics, obtained at temperatures lower than T_0 are shifted to the right, the others are shifted to the left. The master curve describes the material behaviour at a much larger time range than the time range used in the measurements. In this example, vertical shifts are neglected.

This principle can be applied when the overlapping parts of the characteristics in the master curve match. The master curve must be smooth without discontinuities.

4.3.2 Criteria, derived with use of generalised Maxwell model

To obtain master curves and to investigate properly the applicability of this principle upon brain tissue, it is necessary to describe the mechanical behaviour of the material with a constitutive model. In section 3.1 it is assumed that brain tissue behaves as a linear viscoelastic material so the generalised Maxwell model for solids is used to describe the constitutive behaviour. A simplifying assumption is that the inspected material consists of one component. In the next subsection, the temperature-dependent behaviour of composites is discussed. A description of the generalised Maxwell model for solids is given in section 3.2.

For polymers the following relations between the relaxation time τ and shear modulus G and the temperature T can be derived, using molecular theories (Ferry, 1980):

$$\frac{\tau(T)}{\tau(T_0)} = a(T,T_0) \tag{4.8}$$

$$\frac{G_i(T)}{G_i(T_0)} = \frac{1}{b(T,T_0)} \tag{4.9}$$

When the reference temperature T_0 has been chosen, the shift functions $a_T = a(T,T_0)$ and $b_T = b(T,T_0)$ depend only on the difference between T and T_0. The relaxation modulus $G(t,T)$ for one Maxwell element can be rewritten by:

$$G(t,T) = G_i(T)exp(-\frac{t}{\tau_i(T)}) = G_i(T)\frac{G_i(T_0)}{G_i(T_0)}exp(-\frac{t}{\tau_i(T)}\frac{\tau_i(T_0)}{\tau_i(T_0)}) =$$

$$= \frac{1}{b_T} G(\frac{t}{a_T}, T_0) \tag{4.10}$$

This equation relates the relaxation modulus at a temperature T to the relaxation modulus at the reference temperature T_0. For a generalised Maxwell model the relation between $G(t,T)$ and $G(t,T_0)$ is the same.

The significance of this equation can be explained with use of an isothermal set of characteristics for the relaxation modulus measured on a limited frequency range. If the shift functions a_T and b_T are known, each characteristic for $G(t,T)$ can be plotted as $b_T G(t,T)$ against t/a_T. One master curve is constructed that corresponds to temperature T_0 with a frequency range that may be much wider than the limited range used in the measurements.

A set of isothermal characteristics can also be used to estimate the shift functions by constructing the master curve. This construction for a set of isothermal relaxation moduli is performed in three steps:

1. Make an arbitrary choice for the master curve to which the others are shifted to. The corresponding temperature is referred to as the reference temperature.

2. Inspecting (4.10), associated with (4.9) and (3.8) it is found that the temperature dependence of horizontal asymptote (for $t \to \infty$) of the relaxation curve, $G_\infty(T)$, can be described by the shift function b_T alone (thus independent of a_T). The asymptotes for all characteristics are vertically shifted to the level of the asymptote of the master curve. This shift is performed manually and the levels are compared by visual inspection. These shifts yield the shift functions b_T.

3. The shift functions a_T are determined, after the vertical shift is applied, by horizontally shifting the characteristics till it is concluded by visual inspection that the shapes of the overlapping parts of the characteristics match well.

The expression for the storage modulus, (3.3), can be rewritten as:

$$\begin{aligned} G'(\omega,T) &= G_i(T)\frac{\omega^2\tau_i^2(T)}{1+\omega^2\tau_i^2(T)} = G_i(T)\frac{G_i(T_0)}{G_i(T_0)}\frac{\omega^2 a_T^2\tau_i^2(T_0)}{1+\omega^2 a_T^2\tau_i^2(T_0)} \\ &= \frac{1}{b_T}G'(a_T\omega,T_0) \end{aligned} \tag{4.11}$$

Analogous derivations can be made for the loss modulus, resulting in:

$$G''(\omega,T) = \frac{1}{b_T}G''(a_T\omega,T_0) \tag{4.12}$$

The above derivation is made for a material that is described by one Maxwell element. However, relations (4.11) and (4.12) can also be derived for a generalised Maxwell model.

To estimate the shift functions a_T and b_T with use of the results of dynamic experiments, the loss angle and the dynamic modulus are used:

$$G_d(\omega,T) = \sqrt{G'^2(\omega,T)+G''^2(\omega,T)} = \frac{1}{b_T}G_d(a_T\omega,T_0) \tag{4.13}$$

$$\tan\delta(\omega,T) = \frac{G''(\omega,T)}{G'(\omega,T)} = \tan\delta(a_T\omega,T_0) \tag{4.14}$$

Using the above description, the construction of the master curve and the estimation of the shift factors for a set of isothermal characteristics that are obtained with dynamic experiments, are carried out as described below:

1. Make an arbitrary choice for the characteristics for the dynamic modulus and the loss angle to which the others are shifted to. These characteristics are called the master curves with reference temperature T_0.

2. In (4.14) it is shown that the construction of the master curve of the loss angle depends only on the shift factor a_T. So, the separate characteristics for loss angle δ must be shifted horizontally along the frequency axis onto the master curve to estimate the horizontal shift factor a_T. By visual inspection the matching of the curves is investigated.

3. These horizontal shift factors must be applied to the corresponding characteristics for the dynamic modulus G_d and these must be shifted vertically to the master curve to obtain b_T. Again visual inspection is used to investigate the matching.

In this way, the vertical and horizontal shift factors can be estimated separately for dynamic experiments.

For both dynamic and relaxation experiments, the shift function a_T is associated with a horizontal shift and b_T is associated with a vertical shift of a characteristic towards the master curve. Therefore these shift functions are referred to as horizontal, vertical shift functions, respectively.

As was already mentioned in section 4.3.1, the application of the principle is allowed when the shifted characteristics match with the master curve at the overlapping part of the frequency or time scale. Using the generalised Maxwell model, this criterion can be related to the relaxation times. When the time-dependent behaviour of the material is described by only one relaxation time, this criterion is always true. When more relaxation times are used, the temperature dependence for all relaxation times has to be equal to obtain a good match of the various characteristics (Oomens, 1993).

The second condition that has to be fulfilled, concerns the shift functions for the various viscoelastic functions. By different experimental methods various viscoelastic characteristics can be estimated. The application of the time/temperature superposition principle on one isothermal set of characteristics results in the shift functions. The principle can also be applied on characteristics for other viscoelastic functions. It follows from (4.8) and (4.9) that for a material, described by a generalised Maxwell model, the application has to lead to the same shift functions if the same reference temperature has been chosen.

The third condition is formulated on the basis of experience. It is widely noticed that the shape of ${}^{10}\log(a_T)$ as a function of the temperature is smooth without discontinuities. Further, by experience it is concluded that often the relation between a_T and the temperature can be described by the Williams-Landel-Ferry (WLF) equation (see Ferry (1980), p. 280 and further) or an Arrhenius equation (see Oomens (1993)). The WLF-equation is used when the temperatures are between the glass temperature T_g and $T_g + 100$ K, for higher temperatures the Arrhenius equation is used. To allow the application of the principle, a_T has to be fitted with a known function, preferable with the WLF- or Arrhenius equation.

Materials that satisfy these three conditions (good matching of the overlapping parts of the characteristics, a_T described by a smooth function, equal shift for all viscoelastic characteristics) and therefore follow the time/temperature superposition principle are called *thermorheologically simple.*

4.3.3 Biological tissues

Till now the application of the time/temperature superposition principle has been only discussed for a material consisting of one component that displays linear viscoelastic behaviour. However, biological tissues are composites and display often physically nonlinear behaviour.

When the principle is applied to a material that consists of various linear viscoelastic polymers, complications arise. To explain these complications it is assumed that each component can be described by a generalised Maxwell model and that the principle can be applied on the separate components. If the temperature dependence of the separate components can be described by the same shift factors the principle can also be applied to a composition of these materials. When the shift factors differ, the application of the principle on a composition of the materials is not allowed.

The most straightforward method to investigate whether a difference exists, is to estimate and compare all shift functions of the individual components with dynamic experiments in the used frequency range. Unfortunately, the chemical composition of brain tissue is too complex to start an investigation of the applicability on each separate component.

A simpler but less accurate method is to compare the shift functions of the material, estimated from dynamic shear experiments with the shift functions, estimated from relaxation experiments. In this way, the shift functions are estimated on different parts of the relaxation time range because the relevant relaxation times for relaxation experiments differ from the relevant relaxation times for dynamic experiments (see section 4.1). If these shift functions do compare, an indication is found that the shift factors for the various components are comparable. Full certainty cannot be obtained by the second method, because only a limited part of the relaxation time range is investigated.

In section 3.1 the constitutive behaviour of brain tissue was assumed to be linear viscoelastic. The results, presented in section 4.2.1 confirmed this simplification. This means that the application of the principle could be tested on brain tissue without concerns about physical nonlinearities.

Till now, no publications have been found that contain a discussion about the use of the time/temperature superposition on a biological tissue. Therefore, the use of the time/-temperature superposition principle on brain tissue must be verified. Four criteria have to be fulfilled:

1. The overlapping parts of the shifted characteristics must match,
2. Same temperature dependence for all viscoelastic functions,
3. The relation between the horizontal shift factors and the temperature must be described with a known function (for example the WLF or Arrhenius equation),
4. Same temperature dependence for all components.

The following three actions are used to examine those criteria:

1. Visual inspection of the matching of the adjacent curves at the overlapping part of the time or frequency range,
2. Comparison of the shift functions, obtained from dynamic shear experiments with those, obtained from shear relaxation experiments,

3. Visual inspection of the shape of the curve for a_T as a function of the temperature and examination of the quality of the fit of an Arrhenius equation and WLF-equation. Both equations are used because the glass temperatures for the separate components in brain tissue are unknown.

The second action is used to examine the differences in a_T for different viscoelastic functions and to investigate the differences in a_T due to the various components in brain tissue. If the difference between both estimated shift functions a_T is large, the temperature dependent behaviour of the material cannot be described by the theory, developed in this section.

4.3.4 Experimental aspects

The temperature of the samples has to be changed during the experiments. To obtain a master curve describing the constitutive behaviour at frequencies higher than the limited range used in the experiments, the temperature has to be decreased. However, if the temperature of a sample is not equal to body temperature of the donor, irreversible changes in the structure of brain tissue can occur. When the rectal temperature of a human exceeds 41°C for prolonged times, some permanent brain damage results due to, for example, solidifying of proteins (Ganong, 1981). If the temperature of a biological tissue is below 0°C , water in that tissue will freeze. In both cases the structure of the tissue is altered permanently. Information about structural changes in biological tissues due to temperature variations in the range 5–40°C is not found.

The brain tissue is stored for at least 24 hours at a temperature of 7°C. Probably, structural changes due to the low temperature in the refrigerator have already occurred during this storage. The temperature during the experiments to investigate the application of the principle, will be varied stepwise between 7 and 37°C. Lower temperatures will not be used.

To control the temperature of the sample between the plates on the RFS II, a sensor was placed just below the centre of the sample in the lower flat plate. When the measured temperature differs from the selected temperature, a liquid is used to bring the lower plate on the selected temperature. This is a slow process, because first the liquid has to be brought onto the selected temperature and secondly, the lower plate has to adopt this temperature. A temperature rise of 7°C takes at least 10 minutes. To obtain a set of characteristics at five different temperatures between 7°C and 37°C takes about 2 hours. During this time it is possible that the mechanical properties of the samples change due to, for example, dehydration. These changes are already indicated in section 4.2.2.

To investigate the influence of the time span during which the sample is situated on the RFS II and to examine the structural changes, measurements must be compared, taken before and after the temperature variations. Of course, these measurements must be done at the same temperature.

4.3.5 Application of the principle on brain tissue

The set in fig. 4.6 is used to demonstrate the results of the shift process. Information about the used sample can be found in appendix E. In table 4.1 the elapsed time from the start of the first measurement and the used temperature of the individual isothermal characteristics are shown. At each temperature a relaxation and a dynamic shear experiment were carried out with a strain amplitude of 1%. Visual inspection of the data indicates that the measured viscoelastic properties of brain tissue depend on the temperature of the sample.

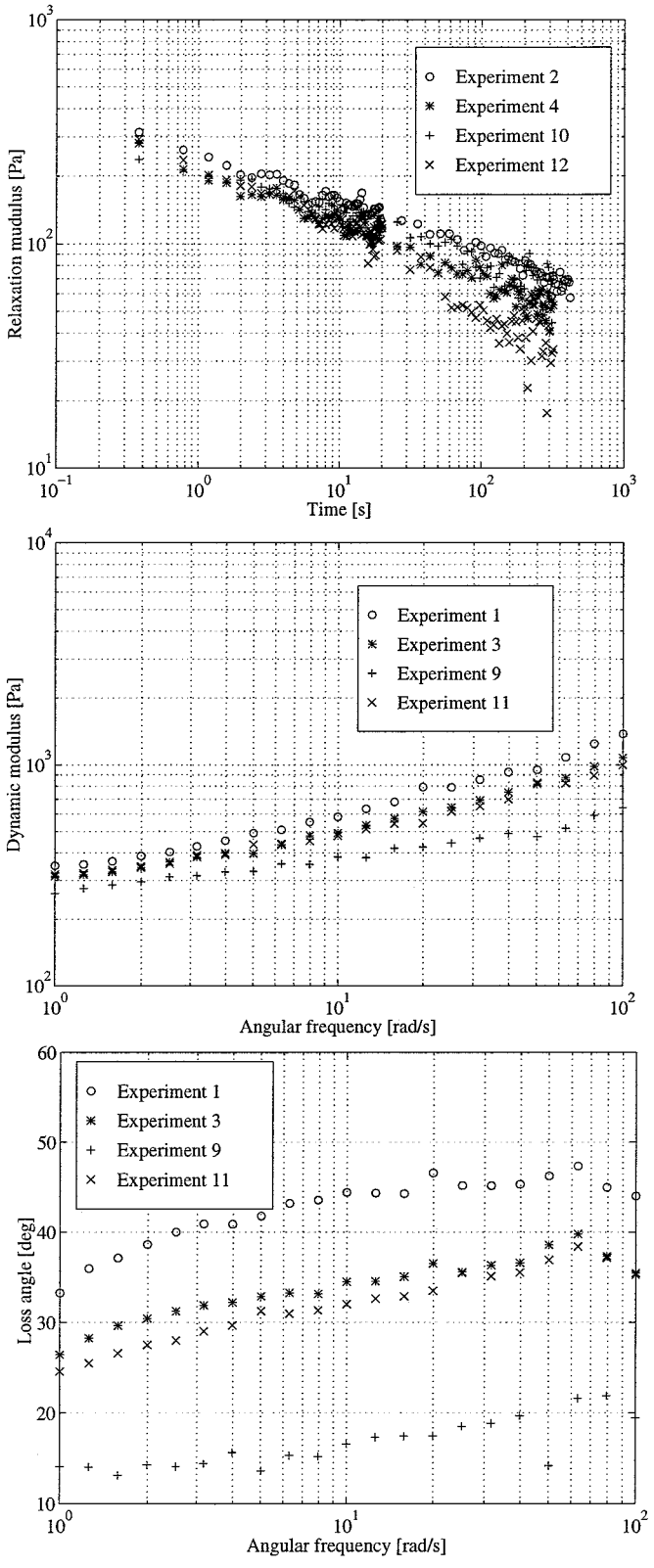

Figure 4.6: Isothermal curves for the relaxation modulus, the dynamic modulus and the loss angle. Elapsed time and temperature are listed in table 4.1.

Table 4.1: Temperature and time, elapsed from the first experiment, of isothermal dynamic and relaxation measurements.

experiment number	Dynamic (D) or Relaxation (R)	temperature (°C)	elapsed time (min)
1	D	5.9 ± 0.8	0
2	R	8.1 ± 0.9	10
3	D	14.6 ± 0.2	30
4	R	15.1 ± 0.1	35
5	D	23.9 ± 0.2	50
6	R	22.8 ± 0.4	55
7	D	30.7 ± 0.3	65
8	R	29.2 ± 0.7	75
9	D	37.8 ± 0.3	90
10	R	37.0 ± 0.6	95
11	D	13.9 ± 0.2	110
12	R	15.2 ± 0.9	115

First, experiment no. 3 was compared with 11 and experiment no. 4 with 12 to investigate whether irreversible changes can be detected after a temperature rise and decrease from 14°C to 37°C. Fig. 4.6 shows that the differences between the characteristics for the loss angle and the dynamic modulus around 14°C are much less than the differences between the curves obtained at other temperatures. The curves for the relaxation modulus are more difficult to compare, because the spread in the data points of each curve has the same magnitude as the differences between the separate curves. However, considering the dynamic measurements, it is concluded that no important irreversible structural changes in the mechanical behaviour of the sample have occurred.

Following the procedure presented in section 4.3.1, first the isothermal loss angle curves are shifted horizontally manually to the reference curve, using a computer program that has been written by Zoetelief (1992). The reference temperature is chosen to be 37.8°C (experiment no. 9) because this temperature approximates the body temperature of the donor. Then, after the shift factor a_T is applied to the dynamic moduli, the shift factor b_T is estimated by shifting the dynamic modulus curves to the reference curve. Both master curves are presented in fig. 4.7. Visual inspection of the master curves did not lead to any grounds to reject the use of the time/temperature superposition principle. The first condition, good matching to the adjacent curves, seemed to be fulfilled.

The shift functions have to be compared with those, obtained by using the relaxation curves. Unfortunately, the relaxation curves, shown in fig. 4.6 do not end in a horizontal asymptote, although the experiments were continued till the lower limit of the torque transducer of the RFS II was reached (G_∞ cannot be determined). So, a vertical shift to estimate the shift factor b_T cannot be applied. It was decided to fit a curve through the vertical shift function b_T, estimated with the dynamic experiments. In this way, the vertical shift factors could be estimated and applied to the relaxation curves. Peters (1995) suggested the use of an exponential function to fit the curves:

$$b_{T,fit}(T, T_{0,dynamic}) = c_1 \exp(-T/c_2) \tag{4.15}$$

where c_1 and c_2 are constants. The obtained fit is shown in fig. 4.9 together with the shift functions b_T, estimated with the dynamic moduli and the used values from the fit for the relaxation experiments. As shown in table 4.1 the reference temperatures for the relaxation and dynamic experiments differ about 0.8°C. This is caused by the temperature control system (see section 4.3.4). An error will be made by using this fit for the relaxation experiments (discussion see below).

After the vertical shift has been applied to the relaxation modulus, the shift function a_T is determined by a horizontal shift, as explained in section 4.3.1. The obtained master curve for the relaxation modulus is shown in fig. 4.7. On visual inspection it is concluded that the master curve is smooth without discontinuities.

In fig. 4.8 the horizontal shift factors are shown versus the temperature for both the dynamic and the relaxation experiments. The spread of the individual factors is large. An error in the shift process of a curve of the dynamic experiments does affect all subsequent shifts and each subsequent estimated factor has a larger error than it's predecessor. Further, an error in estimating a_T for dynamic experiments does affect b_T and even a_T for relaxation experiments. A rough estimation of the spread in ${}^{10}\log(a_T)$ is performed by repeating the shift process several times for the same isothermal set. These repeats led to a value of 0.3 at 31°C to 1 for 8°C due to the manual shift. This means that the error in the horizontal shift is about one decade for the characteristic obtained at 8°C. Another error is caused by the use of a fit for the vertical shift function to shift the curves for the relaxation moduli. However, it is assumed that this error can be neglected in comparison to the errors caused by the shift process. When the spread for ${}^{10}\log(a_T)$ is represented by error bars in fig. 4.8, it is found that these error bars for the horizontal shift functions of the dynamic and relaxation experiments do overlap. The third criterion, consistency of the temperature dependency of the horizontal shift with experience, is examined by two means. First, due to the small number of isothermal curves and the large spread in the individual shift factors, it is difficult to draw conclusions about the smoothness of the curve for a_T versus the temperature. However, strong discontinuities that would reject the use of the principle, are not observed. Secondly, the estimated shift functions were fitted with the Arrhenius and WLF-equation. In fig. 4.8 the Arrhenius fit is shown. The fit looks very reasonable (correlation coefficient $C = 0.94$). The fit with the WLF-equation was very poor ($C < 0.25$).

Ferry (1980) suggested that the vertical shift factor b_T can be related to density variations due to temperature changes:

$$b_T = \frac{\rho T}{\rho_0 T_0} \tag{4.16}$$

where ρ_0 and ρ are the density at T_0 and T (in Kelvin), respectively. The density of brain tissue as function of the temperature is not measured. As stated in table A.1 brain tissue consists of water for about 80% so an approximation for b_T as a function of the temperature is made by using the density of water. The density of water varies between 999.97 kg/m^3 at 278 K and 993.3 kg/m^3 at 310 K. In fig. 4.9 relation (4.16) can be compared with the empirically estimated values for b_T. Definitive conclusions about the obtained vertical shifts cannot be drawn, because the density for brain tissue as function of temperature has to be known.

Five sets of isothermal curves for the relaxation and dynamic moduli and the loss angle were obtained. A new sample was used for each set, originating from another region in the brain. For all these samples, it was possible to construct smooth master curves. Always a fit for the vertical shift function was used to apply the principle on relaxation experiments.

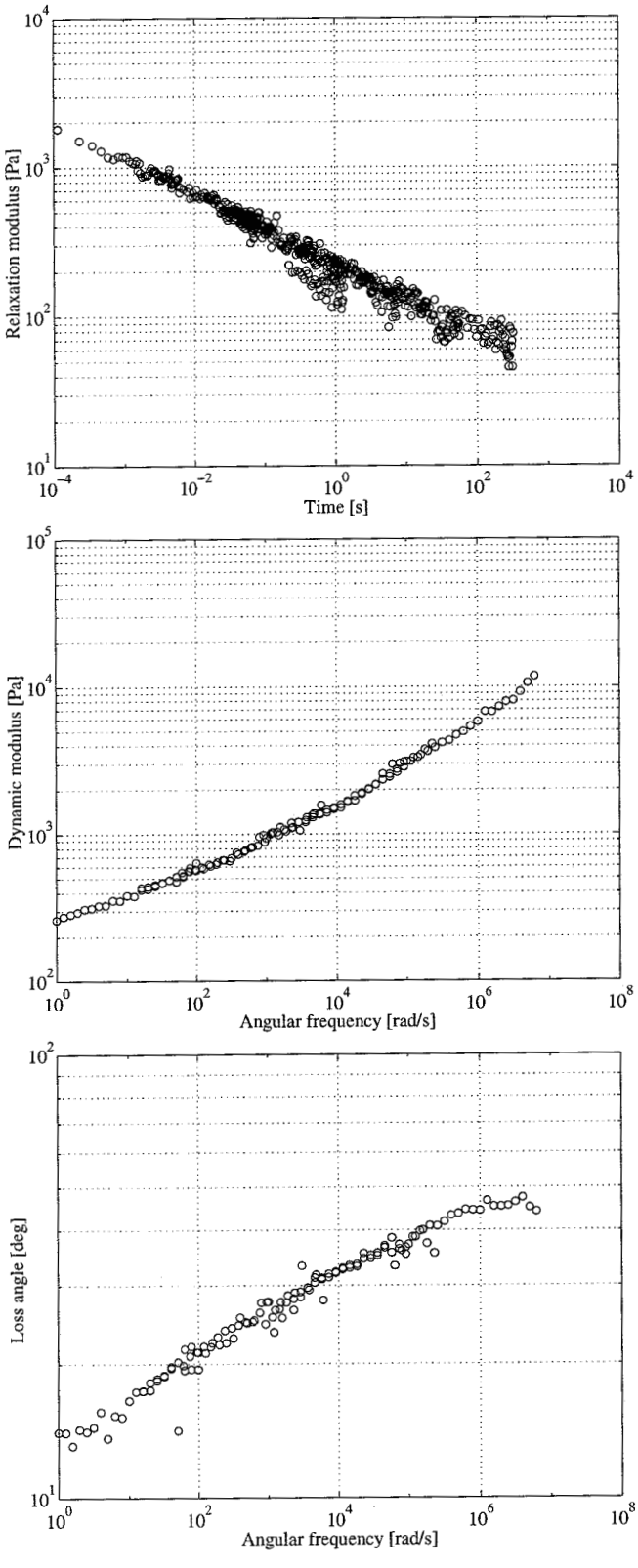

Figure 4.7: Master curves for the relaxation modulus, the dynamic modulus and the loss angle.

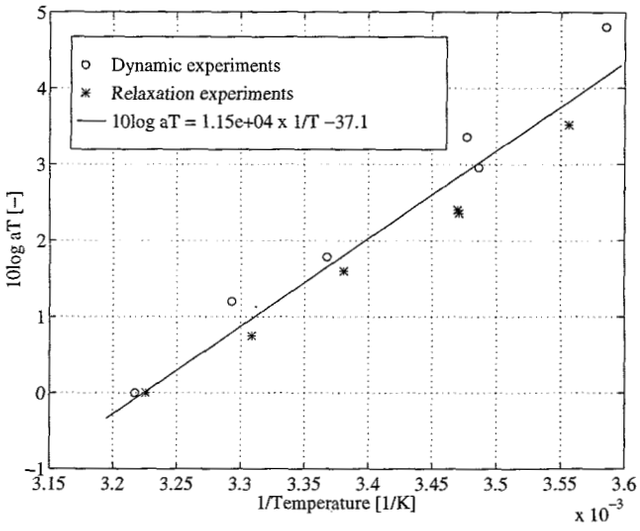

Figure 4.8: The horizontal shift function a_T estimated from the dynamic and relaxation experiments, plotted together with an Arrhenius fit.

Table 4.2: Overview of the estimated Arrhenius equations for the shift functions a_T

number of isothermal set	slope (10^3 1/K)	intercept (-)	correlation coefficient
1	2.7 ± 0.3	-9 ± 1	0.85
2	4.5 ± 0.3	-14.6 ± 0.9	0.97
3	8.5 ± 0.6	-27 ± 2	0.96
4	8 ± 1	-25 ± 3	0.89
5	11.5 ± 0.9	-37 ± 3	0.94

Error bars of the horizontal shift functions were estimated from relaxation and dynamic experiments. These do overlap in all cases, although they were large. The horizontal shift functions were fitted with an Arrhenius equation with a correlation coefficient between 0.85 and 0.95 (see table 4.2). For all five samples, the criteria, as formulated in section 4.3.3, were satisfied.

The aim of the application of the time/temperature superposition is to obtain viscoelastic characteristics for frequencies above 15.9 Hz. As can be seen in fig. 4.7 the maximum of the frequency range for the master curves is about 10^6 Hz, a range sufficiently large to describe the behaviour of brain tissue for frequencies relevant in impacts. The master curves for the other samples have a comparable frequency range.

4.3.6 Conclusions

To investigate the applicability of the time/temperature superposition principle, three criteria are formulated for a material that consists of one component on the basis of the generalised Maxwell model for solids and conform experimental experiences. These criteria are good matching of the shifted characteristics, equal shift functions for the relaxation and dynamics

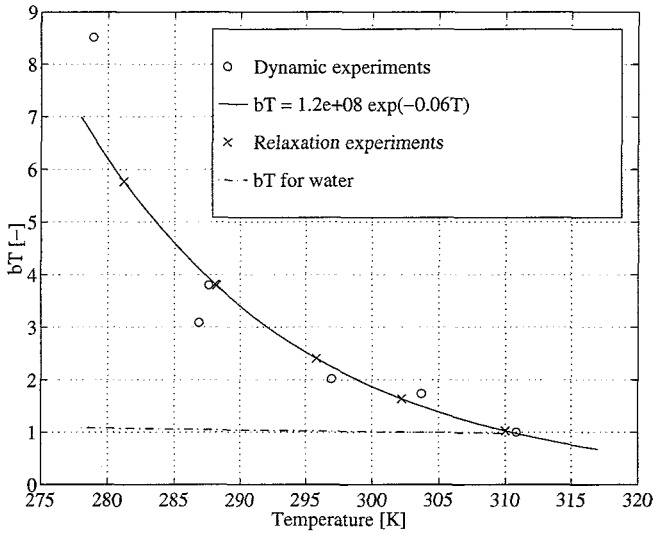

Figure 4.9: The vertical shift function b_T estimated from the dynamic experiments, the fit and the used values for the relaxation experiments.

experiments and the horizontal shift function must be fitted with known function. Because brain tissue is a composite, an extra criteria is added (equal shift functions for the separate components).

Five samples, originating from different parts of a calf brain, were used to obtain isothermal sets of the relaxation modulus (measured till the torque was equal to lower limit of RFS II) and the dynamic modulus and the loss angle (frequency range 0.159–15.9 Hz) at strains of 1%. The used temperature range was 7–37°C. It was possible to construct master curves for the relaxation modulus, the dynamic modulus and the loss angle. The criteria were investigated by visual inspection of the smoothness of the master curves, comparison of the obtained horizontal shift functions and fitting the horizontal shift functions with the WLF-equation. The four criteria were satisfied for all samples so no arguments were found to reject the application of the principle upon brain tissue. The master curves, obtained with the dynamic experiments, display the viscoelastic properties for a large frequency range (between 1 and 10^6 Hz). This range is sufficient to describe the mechanical behaviour at frequencies relevant in impacts.

The shifts were performed by visual interaction with a computer program. The uncertainty for the horizontal shifts along the time or frequency axis for the characteristics are cumulative. For the characteristics, measured at the lowest temperatures, the uncertainty are about one decade on the logarithmic time or frequency axis.

The number of five samples is too small to draw final conclusions about the applicability of the time/temperature superposition principle upon brain tissue.

4.4 Comparison between results and literature

The results of the dynamic and relaxation shear experiments, reported in this chapter, can be compared to the published material parameters, listed in table 2.1.

The magnitude of the complex shear modulus, measured with dynamic simple shear experiments at 10 Hz and published by McElhaney et al. (1972) and Fallenstein et al. (1969),

ranges between 600 – 1500 Pa and 500 – 1100 kPa, respectively. In fig. 4.7 the value for the dynamic modulus at 62 rad/s (= 10 Hz) is found to be between 500 and 600 Pa. For the 4 other master curves (not shown in this report) the value varied from 300 Pa to 700 Pa. Like the measurements, described in this report, these experiments were carried out with samples from cerebral white tissue under comparable conditions (high humidity and a temperature of 37°C). However, some aspects as the exact strains used by McElhaney et al. (1972) and Fallenstein et al. (1969) to get the data in table 2.1 are unknown (it is indicated that these were large (> 5%)). The complex shear moduli, reported by Shuck et al. (1970) and Shuck and Advani (1972), are measured at a large frequency range (2–400 Hz). For the whole range, these published values are one or more decade(s) larger than the values given by the master curves, published in this report. However, the used strain and the experimental conditions were not given by Shuck et al.. Finally, the values for the dynamic modulus between 20 and 100 Hz, reported by Bittenbender Arbogast et al. (1995), ranged between 350 and 1000 Pa. The dynamic modulus, measured with the RFS II and shown in fig. 4.7, varied for frequencies between 120 and 630 rad/s (= 20 – 100 Hz) between 600 and 900 Pa. For the other master curves, the value at 120 rad/s varied between 350 and 750 Pa and for 630 rad/s the value ranged from 600 up to 1050 Pa.

The differences and similarities between the results, found in literature and the results, published in this report, cannot be easily explained. The samples were made from different donors, the samples were made from different parts of the brain, the type of experiments was different. Finally, the information as listed in appendix C.2 is not listed completely in these publications.

4.5 General conclusions about the experiments

- The preparation of the individual samples is listed as listed in appendix C.2. Physical linear behaviour was shown for strains between 0.2 and 1%. Further, it was indicated that for strains in this range the enforced torsional shear deformations were geometrically linear. These two aspects were not reported in literature.

- For the first time, an investigation to the application of the time/temperature superposition principle upon a biological is reported. The results satisfied the formulated criteria, a material has to satisfy to allow the application of the time/temperature superposition principle. The frequency range of the master curves, obtained by the dynamic experiments, is sufficient to describe the behaviour of brain tissue for frequencies relevant in impact conditions (20 – 1000 Hz). Only five samples were used, so final conclusions about the applicability of this principle upon brain tissue cannot be drawn.

- The variations in the results are quite large. The measured material parameters, obtained with different samples, differ at most a magnitude of 4. These differences can be related to the errors, made by estimating the dimensions of the samples, to the minimal torque the RFS II is capable to measure and to the construction of the master curves. Further, the differences could be caused by variations in the samples (composition, anisotropy, etc.) but a systematic investigation has not been carried out.

5 Determination of model parameters

As said in chapter 3 brain tissue is considered as a linear viscoelastic material. Therefore the generalised Maxwell model was proposed to describe the constitutive behaviour of brain tissue. In chapter 4 the generalised Maxwell model is successfully used to derive criteria for the application of the time/temperature superposition principle. In this chapter this model will be fitted upon the master curves obtained in the previous chapter. The aim is to compare the results of the relaxation experiments with those of the dynamic experiments and vice versa.

5.1 Results of the fits

When the constitutive behaviour of a material is described by the generalised Maxwell model for solids, relaxation times τ_i and spring constants G_i and G_∞ are used to describe the experimental results as shown in (3.8), (3.9) and (3.10). To obtain these parameters to describe the master curves presented in the previous chapter, a program, based on the nonlinear least squares method of Levenberg-Marquardt, is used (see Zoetelief (1992)). For some situations the method gives negative parameter values. From a mathematical viewpoint this is correct, because it is just a fit, but these negative values are not physically meaningful.

For all five samples the generalised Maxwell model for solids is fitted upon the constructed master curves. For each sample, the number of Maxwell elements to describe the relaxation experiments is estimated independently from the number of elements, used to describe the dynamic experiments. In fig. 5.1 an example is given of the fit of a generalised Maxwell model for solids upon master curves for the relaxation experiments and the dynamic experiments. The calculated parameters are given in table 5.1.

With these parameters, the master curves for the relaxation and dynamical experiments, obtained with the same sample, can be compared. With use of the parameters, estimated by fitting the model upon the master curve for the relaxation modulus, the response for the dynamic modulus and the loss angle is calculated for the frequency range similar to the master curves. The results are presented in fig. 5.2. Next, the parameters, obtained by fitting the model upon the dynamical experiments, are used to calculate the relaxation modulus as function of the time (shown fig. 5.2, too).

The range for the relaxation times obtained with the relaxation experiments is different from the range, obtained with the dynamic experiments as can be seen in table 5.1. When the parameters, obtained with the relaxation experiments, are used to calculate the storage and loss moduli, a deviation can be expected for frequencies higher than 10 kHz because the smallest relaxation time ($11.04 \cdot 10^{-4}$ s) cannot be used to describe these high frequencies.

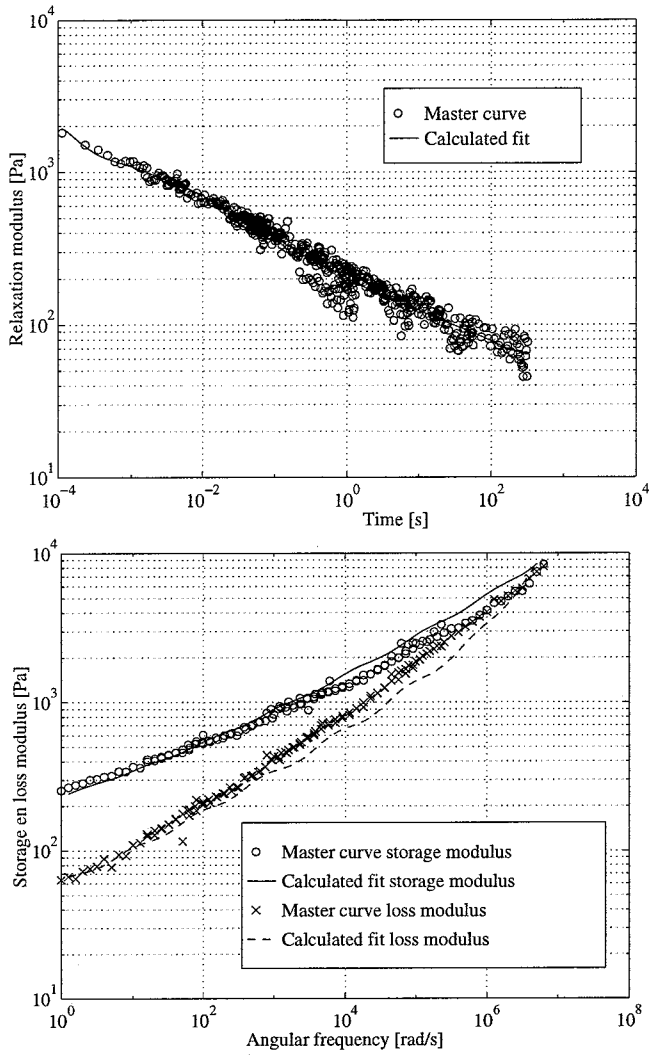

Figure 5.1: The calculated relaxation modulus and the storage and loss modulus, obtained by fitting the generalised Maxwell model for solids upon the relaxation and dynamic experiments, respectively. The parameter values are listed in table 5.1.

This effect is clearly visible in fig. 5.2. A similar deviation can be found for the relaxation modulus, calculated by the parameters that are estimated by fitting the model upon the dynamic experiments. For a time , larger than 1 s the calculations do deviate strongly from the constructed master curve. On the other parts of the time and frequency ranges, the calculated curves do have the same magnitude as the obtained master curves. As stated in section 4.3.5 the errors in the master curves are large (for the characteristic with the lowest temperature, the shift along the frequency axis has an uncertainty of about one decade). The differences between the calculated curves and the measured master curves, shown in fig. 5.2, are much smaller.

5.2 Conclusions

- The obtained master curves for the relaxation modulus and the storage and loss moduli are fitted with the generalised Maxwell model for solids. The differences between the

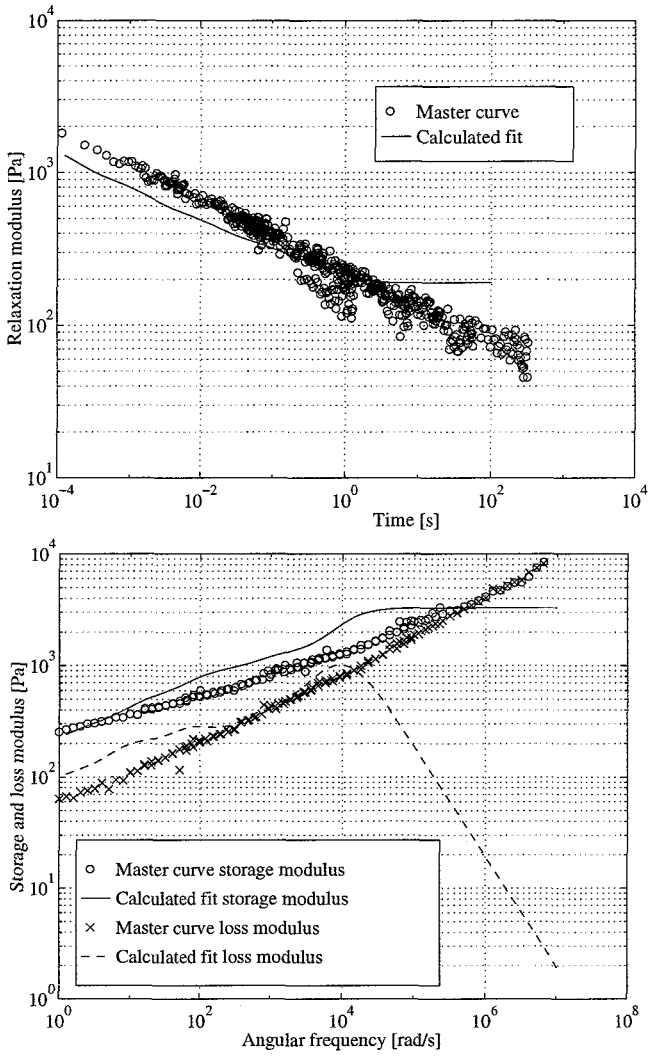

Figure 5.2: The calculated relaxation modulus and the storage and loss modulus using the parameter values obtained by fitting the generalised Maxwell model for solids upon the dynamic experiments and relaxation experiments, respectively. The parameter values are listed in table 5.1.

fits and the master curves are smaller than the errors induced by the shift process.

- Comparison of the parameters was performed by calculating the relaxation modulus with parameters, obtained by fitting the model upon the storage and loss moduli and vice versa. The results showed that on relevant parts of the time and frequency range the experimental results were comparable. The differences were smaller than the errors, mentioned in section 4.2.3 and section 4.3.5

- Therefore, the use of a one-dimensional generalised Maxwell model for solids is sufficient to describe the constitutive behaviour of brain tissue in torsional shear experiments for small deformations.

Table 5.1: Model parameters obtained by fitting the generalised Maxwell model for solids upon master curves

model fitted upon relaxation modulus		model fitted upon dynamic modulus and loss angle	
G_i (Pa)	τ_i (s)	G_i (Pa)	τ_i (s)
$1.97 \cdot 10^3$	$1.04 \cdot 10^{-4}$	$3.49 \cdot 10^4$	$4.89 \cdot 10^{-8}$
$3.95 \cdot 10^2$	$1.28 \cdot 10^{-3}$	$3.11 \cdot 10^3$	$1.15 \cdot 10^{-6}$
$3.84 \cdot 10^2$	$1.27 \cdot 10^{-2}$	$1.61 \cdot 10^3$	$1.16 \cdot 10^{-5}$
$2.52 \cdot 10^2$	$9.49 \cdot 10^{-2}$	$8.05 \cdot 10^2$	$1.23 \cdot 10^{-4}$
$1.24 \cdot 10^2$	$7.63 \cdot 10^{-1}$	$4.14 \cdot 10^2$	$1.24 \cdot 10^{-3}$
$6.39 \cdot 10^1$	7.47	$2.22 \cdot 10^2$	$1.12 \cdot 10^{-2}$
$5.05 \cdot 10^1$	$7.98 \cdot 10^1$	$1.27 \cdot 10^2$	$9.28 \cdot 10^{-2}$
		$9.60 \cdot 10^1$	$8.46 \cdot 10^{-1}$
G_∞		G_∞	
(Pa)		(Pa)	
$6.37 \cdot 10^1$		$1.90 \cdot 10^2$	

6 Conclusion and recommendations

6.1 Conclusions

- With torsional shear experiments it was shown that the mechanical behaviour of brain tissue is physical linear for conditions, indicated to be geometrically linear. The results were not reproducible.
- Investigation to the applicability of the time/temperature superposition principle upon brain tissue showed that criteria, formulated on the basis of the generalised Maxwell model for solids and common experiences, were satisfied.
- The constructed master curves describe the mechanical behaviour of brain tissue for frequencies relevant to impact conditions.
- The comparison of the separate fits of the generalised Maxwell model for solids upon these master curves showed that, for each sample, the differences between the results of the relaxation experiments and the dynamic experiments can be neglected in comparison to the uncertainties estimated for the master curves.

6.2 Recommendations

Recommendations for the torsional shear experiments:

- With a histological investigation the influence of the experiments upon the structure in a sample can be investigated. The internal structure of two samples can be compared, both originating of the same cylinder. One sample is used in an experiment, the other is investigated without being used in an experiment. Further, histological investigation can be used to estimate any predominant direction of the fibres in a sample and the number and direction of the blood vessels. With the results of these examinations, the measurements with different samples can be compared and indications can be given for different mechanical responses of the various samples.
- More certainty about the linearity of the relation between the enforced angular displacement and the measured torque response can be obtained by sampling the response and fit this signal with a sinus (frequency same as enforced displacement) or analysis it by the application of a Fourier transformation. Further, a thorough analytical analyse of the deformation can prove whether the enforced deformations are geometrically linear.

Recommendations to obtain more certainty about the applicability of the time/temperature superposition principle upon brain tissue:

- Estimation of the density of brain tissue as function of the temperature is necessary to investigate the suggested relation between the vertical shift function b_t and the density. If b_T cannot be related to the density of the brain tissue, another theory has to be used to explain the vertical shift function b_T, probably based upon interactions between the various components.
- It is not useful to investigate the applicability upon separate components of brain tissue. First, the number of individual components of brain tissue is very large. Secondly, some components may interact with each other, changing their temperature-dependent behaviour. Therefore, results of the investigation to the separate components cannot be used to characterise the temperature-dependent behaviour of the composite.
- It is recommended to change the temperature control system of the RFS II, to shorten the time used to obtain the isothermal characteristics. Heating and cooling by circulating hot and cold air in the moist chamber is an option. It must be checked if the temperature sensor in the lower plate can be used as an indication for the temperature in the sample.
- To decrease the uncertainties in the shift functions, a mathematical method has to be found to obtain an indication for the optimal overlap when one characteristic is shifted towards the second.

More general remarks about the project:

- To estimate the similarities and differences between *in vivo* and *post mortem* conditions indentation experiments can be performed just before and after the sacrifice of the donor. Indentation experiments can also be used, to compare the mechanical behaviour of brain tissue in *in situ* with *in vitro* conditions.
- As stated in section 2.1.4 it is unknown if the mechanical properties of calf brains are equal to the properties of human brains. Therefore, the same experiments has to be performed with human brains.
- To investigate the inhomogeneity of brain tissue or to estimate anisotropic behaviour, the torsional shear experiments are not suitable. Two-dimensional rotation experiments can be used to investigate the deformations to a sudden acceleration. A cylinder shaped brain tissue sample is placed inside a cylinder and accelerated about it's axis. The deformations can be made visible by using markers on the surface and tracing them with help of a high speed camera.
- Wave propagation through brain tissue can be examined by using sound waves. However, the application of wave propagation to estimate material parameters is complicated, due to the complex geometry and the viscoelasticity of the brains.

Bibliography

Barber, T., Brockway, J. and Higgins, L., 1970, "The density of tissues in and about the head", *Acta Neurol. Scandinav.*, 46, 85–92.

Bittenbender Arbogast, K., Meaney, D. and Thibault, L., 1995, "Biomechanical characterization of the constitutive relationship for the brainstem", in *Proc. 39th Stapp Car Crash Conf.*, pp. 153–159.

Bylski, D., Kriewall, T., Akkas, N. and Melvin, J., 1986, "Mechanical behavior of fetal dura mater under large deformation biaxial tension", *J. Biomechanics*, 19, 19–26.

Chatfield, C., 1989, *Statistics for technology.* Chapman and Hall, London, Great Britain, 3rd edn.

Claessens, M., 1994, "Anatomical description of the human head", Tech. Rep. WFW 94.003, Department of Mechanical Engineering, Eindhoven University of Technology, The Netherlands.

Dodgson, M. C. H., 1962, "Colloidal structure of brain", *Biorheology*, 1, 21–30.

Duck, F., 1990, *Physical properties of tissue.* Academic Press, London, Great Britain.

Estes, M. S. and McElhaney, J. H., 1970, "Response of brain tissue to compressive loading", in *ASME Paper No. 70-BHF-13.*

Fallenstein, G., Hulce, V. and Melvin, J., 1969, "Dynamic mechanical properties of human brain tissue", *J. Biomechanics*, 2, 217–226.

Ferry, J., 1980, *Viscoelastic properties of polymers.* John Wiley & Sons, New York, NY, USA.

Findley, W., Lai, J. and Onaran, K., 1976, *Creep and relaxation of nonlinear viscoelastic materials.* North-Holland Publishing Company, Amsterdam, The Netherlands.

Galford, J. E. and McElhaney, J. H., 1970, "A viscoelastic study of scalp, brain and dura", *J. Biomechanics*, 3, 211–221.

Ganong, W., 1981, *Review of Medical Physiology.* Lange Medical Publications, Los Altos, CA, USA.

Holbourn, A. H. S., 1943, "Mechanics of head injuries", *The Lancet*, 9, 438–441.

Hubbard, R. P., 1971, "Flexure of layered cranial bone", *J. Biomechanics*, 4, 251–263.

Hubbard, R. P., Melvin, J. and Barodawala, I., 1971, "Flexure of cranial sutures", *J. Biomechanics*, 4, 491–496.

Hunter, S. C., 1983, *Mechanics of continuous media.* Ellis Horwood Ltd., 2nd edn.

Jaslow, C. R., 1990, "Mechanical properties of cranial sutures", *J. Biomechanics*, 23(4), 313–321.

Kaplan, N. and Koprowski, H., 1973, "Laboratory technics in rabies", Tech. rep., WHO, Geneve, Switzerland.

Koiter, W., 1985, *Inleiding tot de leer van stijfheid en sterkte (in Dutch).* Epsilon Uitgaven, Utrecht, The Netherlands.

Kriewall, T., Bylski, D., Melvin, J. and Work, B., 1983, "Mechanical behavior of fetal dura mater under large axisymmetric inflation", *J. Biomechanical Engineering*, 105, 71–76.

Liu, Y. K., Chandran, K. B. and Wickstrom, J., 1976, "In vivo dynamic material properties of the canine spinal cord", in *Proc. 29th ACEMB*, p. 48.

Ljung, C., 1975, "A model for brain deformation due to rotation of the skull", *J. Biomechanics*, 8, 263–274.

Macosko, C., 1994, *Rheology: Principles, Measurements and Applications.* VCH Publishers, New York, NY, USA.

Margulies, S. S., 1987, *Biomechanics of traumatic coma in the primate*, Ph.D. thesis, University of Pennsylvania, USA.

McElhaney, J., Fogle, J., Bryars, E. and Weaver, G., 1964, "Effect of embalming on the mechanical properties of beef bone", *J. Applied Physiology*, 6, 1234–1236.

McElhaney, J. H., Fogle, J. L., Melvin, J. W., Haynes, R. R., Roberts, V. L. and Alem, N. M., 1970, "Mechanical properties of cranial bone", *J. Biomechanics*, 3, 495–511.

McElhaney, J. H., Melvin, J. W., Roberts, V. L. and Portnoy, H. D., 1972, "Dynamic characteristics of the tissue of the head", in *Symp. Perspectives in Biomedical Engineering*, pp. 1–8.

McElhaney, J. H., Stalnaker, R., Estes, M. and Rose, L., 1969, "Dynamic mechanical properties of scalp and brain", in *Rocky Mountain Bioengineering, Proc. 6th annual symposium*, pp. 67–73.

McGarvey, K. A., Lee, J. M. and Boughner, D. R., 1984, "Mechanical suitability of glycerol preserved human dura mater for construction of prosthetic cardiac valves", *Biomaterials*, 5, 109–117.

McIlwain, H., 1966, *Biochemistry and the central nervous system.* J. & A. Churchill Ltd., London, Great Britain, 3rd edn.

McMinn, R., Hutchings, R. and Logan, B., 1994, *Colour atlas of head and neck anatomy.* Mosby-Wolfe, London, Great Britain, 2nd edn.

Melvin, J., Robbins, D. and Roberts, V., 1969, "The mechanical behaviour of the diploe layer of the human skull in compression", in *Proc. 11th Midwestern Mechanics Conf.*, pp. 811–818.

Mendis, K. K., 1992, *Finite element modeling of the brain to establish diffuse axonal injury criteria*, Ph.D. thesis, Ohio state university, USA.

Metz, H., McElhaney, J. and Ommaya, A. K., 1970, "A comparison of the elasticity of live, dead and fixed brain tissue", *J. Biomechanics*, 3, 453–458.

Ommaya, A. K., 1968, "Mechanical properties of tissues of the nervous system", *J. Biomechanics*, 1, 127–138.

Oomens, C., 1993, *Constitutieve modellen (Lecture notes no. 4687, in Dutch).* Eindhoven University of Technology, The Netherlands.

Pamidi, M. R. and Advani, S. H., 1978, "Nonlinear constitutive relations for human brain tissue", *J. Biomedical Engineering*, 100, 44–48.

Peters, G., 1995, Eindhoven University of Technology, Personal communication.

Plantema, F., 1965, *Sandwich construction, The bending and buckling of sandwich beams, plates and shells.* Wiley, New York, NY, USA.

Report of the European Transport Safety Council, 1993, "Reducing traffic injuries through vehicle safety improvements".

Shuck, L., Haynes, R. and Fogle, J., 1970, "Determination of viscoelastic properties of human brain tissue", in *ASME Paper No. 70-BHF-12.*

Shuck, L. Z. and Advani, S. H., 1972, "Rheological response of human brain tissue in shear", *J. Basic Engineering*, pp. 905–911.

Sokal, R. R. and Rohlf, F. J. (eds.), 1981, *Biometry.* W.H. Freeman and Company, San Francisco, CA, USA.

Tunturi, A. R., 1977, "Elasticity of the spinal cord dura in the dog", *J. Neurosurgery*, 47, 391–396.

Vegt, A. V. d., 1992, *Polymeren, van kunststof tot keten (in Dutch).* Delftse Uitgevers Maatschappij, Delft, The Netherlands.

Walsh, E. K. and Schettini, A., 1976, "Elastic behavior of brain tissue in vivo", *Am. J. Physiol.*, 230(4), 1058–1062.

Whorlow, R. (ed.), 1992, *Rheological Techniques.* Ellis Horwood, Chichester, West Sussex, Great Britain.

Wismans, J., Janssen, E., Beusenberg, M., Koppens, W. and Lupker, H., 1994, *Injury biomechanics.* University of Eindhoven, The Netherlands.

Wood, J. L., 1971, "Dynamic response of human cranial bone", *J. Biomechanics*, 4, 1–12.

Zoetelief, W., 1992, "On the numerical simulation of the multilayer injection moulding process", Tech. Rep. WFW 92.100, Department of Mechanical Engineering, Eindhoven University of Technology.

A Anatomy of the human head

This chapter gives a brief introduction to the anatomy of the human head, a more extensive description together with references can be found in Claessens (1994). A detailed photographic overview of the human head can be found in McMinn et al. (1994).

The human skull can be divided in the cranial vault and the facial bone. The cranial vault consists of eight bones. The bones of the skull are connected with complex interlinking surfaces, called sutures. In these sutures, collagenous fibres form bridges between the bones (Jaslow, 1990). Each bone consists of two compact layers (tables) divided by a porous layer, called the diploe layer. In the skull, three different cerebral membranes envelop the central nervous system: the dura mater, the arachnoid and the pia mater. The dura consists of both elastin and collagen fibres. McGarvey et al. (1984) concluded from microscopic pictures that the dura consists of layers with a typical length of 20 μ. Each layer is oriented in a different direction than it's adjacent neighbours yet thoroughly interwoven with them. Probably the tissue can be considered as isotropic on a macroscopic scale.

The cerebral membranes evelop the central nervous system (CNS). Between the membranes and the CNS and in the ventricles of the CNS a liquid, called the cerebrospinal fluid (CSF), is enclosed. The CSF provides nutrients and forms a buffer to protect the CNS. The central nervous system is built of the forbrain (the cerebral hemispheres and the diencephalon), the midbrain and the hindbrain (medulla oblongata, the pons, the cerebellum and the spinal cord). These structures are shown (except the diencephalon) in fig.A.1.

The exterior side of both hemispheres, called the cerebral cortex, is a 1.5 to 4.5 mm thick layer and consists of nerve and support cells. This layer can be recognized by its gray colour and is shaped into folds separated by fissures. The white matter in the hemispheres consists mainly of fibres that connect the cells with other parts of the brain or the central nervous system. The white colour is formed by the myelin shafts that cover the fibres. The two cerebral hemispheres are connected to each other by the corpus callosum.

Just below both hemispheres the diencephalon is located. The major parts of this structure are the thalamus and the hypothalamus. The midbrain forms a fibrous connection between the cerebral hemispheres, the diencephalon and the pons. The pons is connected to the cerebellum and to the medulla oblongata. The latter appears to be continuous with the pons and the spinal cord, placed inside the spinal column.

The pons, the medulla oblongata and the spinal cord consist of gray matter enveloped by white matter. In the lower part of the medulla oblongata fibres cross from the left side to the right side and vice versa, but in the other parts of these three structures the fibres are mainly directed from the spinal cord to the cerebral hemispheres. Anisotropy in these parts of the CNS is possible.

In table A.1 the composition of some parts of the human head is summarised.

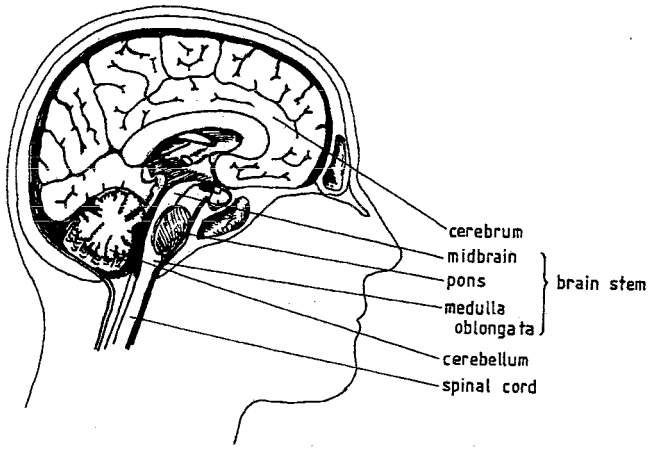

Figure A.1: Schematic overview of the anatomy of the human head (Wismans et al., 1994).

Table A.1: Components of skull bone, cerebrospinal fluid and brain tissue. Values are given as a percentage of fresh wet weight, values between () are mean values (Duck, 1990).

Material	Water (%)	Lipids (%)	Proteins (%)	Other (%)
Cerebrospinal fluid	99	–	0.012–0.043 (0.018)	0.85–1.7 (1.08)
Brain tissue	76.3–78.5 (77.4)	9–17	8–12	1.4–2 (1.5)
gray matter	83–86	5.3	8–12	1.5
white matter	68–77	18	11-12	1.4
Bone tissue				
cortical (tables)	12-15	~ 1	25–26	55-58
trabecular (diploe)	23	~ 1	~ 30	34

B Linear time-dependent relations between stress and strain

A material is linear viscoelastic when two criteria are satisfied:

1. Proportionality: an increase of the excitation results in a proportional increase of the response.
2. Superposition: The response to a set of combined excitations can be described by the sum of the responses to each excitation separately.

Both criteria are used to formulate a general relation between the stress (σ) and strain (γ):

$$\sigma(t) = \int_{-\infty}^{t} G(t-t')\dot{\gamma}(t')dt' \tag{B.1}$$

where $\dot{\gamma} = \partial\gamma/\partial t$ and $G(t)$ is the relaxation modulus. The physical significance of the relaxation modulus is illustrated by a relaxation experiment. In such an experiment the strain is stepwise changed from zero to γ_0 at time $t = 0$ s. The relation for a linear viscoelastic material between stress σ and strain γ is given by

$$\sigma(t) = \gamma_0 G(t) \tag{B.2}$$

For $t \to \infty$ the relaxation modulus $G(t)$ will be equal to G_∞. For liquids, the value will be equal to zero. For solids, G_∞ has a value larger than zero.
For dynamic experiments the the strain is varied harmonically:

$$\gamma(\omega, t) = \gamma_0 \sin\omega t \tag{B.3}$$

where γ_0 is the maximum amplitude of the strain. Then

$$\dot{\gamma}(\omega, t) = \omega\gamma_0 \cos\omega t \tag{B.4}$$

Substituting this equation in (B.1), denoting $t - t'$ by s, results in

$$\begin{aligned}\sigma(\omega,t) &= \int_0^\infty G(s)\omega\gamma_0\cos(\omega(t-s))ds \\ &= \gamma_0 G_\infty + \gamma_0\left[\omega\int_0^\infty (G(s)-G_\infty)\sin\omega s ds\right]\sin\omega t \\ &\quad + \gamma_0\left[\omega\int_0^\infty (G(s)-G_\infty)\cos\omega s ds\right]\cos\omega t\end{aligned} \tag{B.5}$$

The term with $\sin\omega t$ is in phase with γ and the term with $\cos\omega t$ is 90° out of phase. The stress has a periodicity of ω but is out of phase with the strain with a degree depending on the relative magnitudes of these terms. The quantities between the brackets are function of the frequency and independent of time, therefore they are rewritten as

$$G'(\omega) = G_\infty + \omega \int_0^\infty [G(t) - G_\infty] \sin\omega t dt \tag{B.6}$$

$$G''(\omega) = \omega \int_0^\infty [G(t) - G_\infty] \cos\omega t dt \tag{B.7}$$

Now, the stress-strain relation is given by

$$\sigma(\omega, t) = \gamma_0 \left(G'(\omega) \sin\omega t + G''(\omega) \cos\omega t\right) \tag{B.8}$$

The stress can be rewritten to display the amplitude σ_0 and the phase angle $\delta(\omega)$ between the stress and strain.

$$\sigma(\omega, t) = \sigma_0 \sin(\omega t + \delta(\omega)) = \sigma_0 \cos\delta(\omega) \sin\omega t + \sigma_0 \sin\delta(\omega) \cos\omega t \tag{B.9}$$

Comparison between (B.8) and (B.9) shows that

$$G'(\omega) = (\sigma_0/\gamma_0) \cos\delta(\omega) \tag{B.10}$$

$$G''(\omega) = (\sigma_0/\gamma_0) \sin\delta(\omega) \tag{B.11}$$

$$G''(\omega)/G'(\omega) = \tan\delta(\omega) \tag{B.12}$$

The phase angle $\delta(\omega)$ is known as the loss angle, too.

To obtain a complex notation, it is more convenient to change the phase by $\pi/2$:

$$\gamma(\omega, t) = \gamma_0 \cos\omega t \tag{B.13}$$

In this case, the shear stress will be

$$\sigma(\omega, t) = \gamma_0 \left(G'(\omega) \cos\omega t - G''(\omega) \sin\omega t\right) = \sqrt{(G'(\omega))^2 + (G''(\omega))^2} \cos(\omega t + \delta(\omega)) \tag{B.14}$$

Now, a complex stress and strain can be defined

$$\gamma^*(\omega, t) = \gamma_0 \exp(j\omega t) \tag{B.15}$$

$$\sigma^*(\omega, t) = \sigma_0 \exp(j(\omega t + \delta(\omega))) \tag{B.16}$$

Then the complex modulus is defined as

$$\sigma^*(\omega, t)/\gamma^*(\omega, t) = G^*(\omega) = G'(\omega) + jG''(\omega) = (\sigma_0/\gamma_0) \exp(j\delta(\omega) \tag{B.17}$$

$$|G^*(\omega)| = \sigma_0/\gamma_0 = \sqrt{(G'(\omega))^2 + (G''(\omega))^2} \tag{B.18}$$

The absolute value of the dynamic modulus, $|G^*(\omega)|$, is also known as the dynamic modulus $G_d(\omega)$.

C Tissue storage and sample preparation

In this appendix the preparation of samples is discussed. For *in vitro* experiments the preparation can be divided in three parts: the removal of the tissue from the donor, the storage of the tissue and the preparation of the samples. For *in vivo* experiments the laboratory animal has to be prepared as a whole. The preparation methods, found in literature are discussed in the next section. In section C.3, the method is described to prepare the samples, used in the shear experiments discussed in chapter 4.

C.1 Methods obtained from literature study

An important aspect of experiments with biological tissue is the preparation method for *in vitro* experiments or the condition of laboratory animals for *in vivo* experiments. The various storage and preparation methods for brain tissue, dura mater and skull bone, described in literature, are described in section C.1.1. The conditions for the laboratory animals in *in vivo* experiments are discussed in the next subsection. Section C.2 contains a list with items that have to be registered during the preparation process.

C.1.1 Removal and storage methods for *in vitro* experiments

An extended description of a method to remove the brains from a donor is given by Kaplan and Koprowski (1973). This method can be used to obtain dura mater too. Brain tissue was stored at various temperatures (below zero up to 37°C), always in moist conditions. Some articles mentioned the use of a cork bore to cut brain tissue, but it was not described how these bores were used (pushing or rotating). Samples were always immediately used in experiments after the preparation. Dura mater was cut by unknown means. Samples of this tissue were sometimes stored for several weeks in frozen conditions before they were used.

Fallenstein et al. (1969) and McElhaney et al. (1972) remarked that freezing brain tissue resulted in material properties that largely differed from properties determined from samples, made from non-frozen tissues. On the other hand, Bylski et al. (1986) found that results, produced with dura mater samples from fresh tissue were comparable with results obtained from samples of material that had been stored in frozen conditions.

Differences and similarities for brain tissue samples or dura mater samples, stored in various conditions or prepared by different methods, were not discussed in the publications. A systematic analysis of the influence of different preparation methods, storage or experimental conditions cannot be made because the given information is incomplete. A list is drafted that

contains the subjects that have to be registered to obtain a proper registration and to avoid obscurities (see appendix C.2).

To investigate the constitutive relation of skull bone, experiments were performed with beams or cylinders of skull bone from the cranial vault. The bone samples were stored in freezers, embalmed or in closed bottles. Before storing the bone samples were milled, sawed or ground in the desired shapes. The sample origin and orientation in the skull varied, but were indicated by photographs or figures in Jaslow (1990), Wood (1971) and Hubbard et al. (1971). McElhaney et al. (1964) concluded from their measurements that no differences were found between the mechanical properties of embalmed bone and immediate *post mortem* properties. No comparison was made between the properties of frozen bone and fresh bone.

C.1.2 Conditioning of laboratory animals in *in vivo* experiments

Several *in vivo* experiments were performed to investigate the mechanical properties of brain tissue or dura mater. The animals were only slightly sedated (Walsh and Schettini, 1976) or completely anaesthetised ((Liu et al., 1976), (McElhaney et al., 1972) and (Metz et al., 1970)). For the indentation experiments, burr holes were made in the skull and sometimes the dura mater was removed. It is not unknown whether the open holes were kept moist with an isotonic saline or another liquid.

The *in vivo* experiments with dura mater were performed on tissue that envelopes the spinal cord. The spinal column was opened by laminectomy. The dura was kept moist during the experiments.

The temperature during the experiments was not given in any publication. The influence of the used anaesthetics upon the mechanical properties of the investigated tissue was not investigated. Blood pressure was kept normal during the experiments.

C.2 Recommendations for tissue preparation

These items have to be listed for each experiment with a tissue of the human head:

- The age of the donor.
- The medical case history of the donor.
- The cause of death.
- The circumstances (especially the temperature and the time from death till the removal of the brains/membranes) in which the body of the donor has been kept until the brain has been removed.
- In case of *in vitro* experiments:
  - The possible existing damage to the tissue, caused by death or during the removal of the tissue.
  - The conditions like the temperature, the humidity, the use of isotonic saline or Ringers solution and the storage time in which the tissue is kept till the preparation of the samples.
  - The way the samples are made.

  - The place where the sample is taken out of the tissue combined with the orientation, perhaps illustrated with pictures and photos.
  - For brain tissue: the ratio between white and gray matter.

- In case of *in vivo* experiments:
  - The method used to open the skull. Registrate also whether the cerebal membranes are removed.
  - The place where the experiments take place in the brains.

- Important experimental conditions like humidity and temperature.

- To be able to examine whether structural changes has been occured in the sample during the shear experiments, histological investigation has to be performed upon the sample after it has been used in the experiments and upon a sample, originating of the same cylinder but not used in experiments. From the differences and simularities in the tissue structure conclusions can be drawn about the changes induced by the shear experiments.

- Results of histological examination on several samples, used in the experiment, can be used to draw conclusions about the results of the shear experiments (aspects to investigate are for example predominant direction of fibres, ratio between white and gray tissue, blood vessels).

With these noted items it must be possible to compare the measurements of various samples originating from different locations and from different donors.

C.3 Preparation method for shear experiments

To be capable to perform shear experiments with brain tissue on the RFS II with plate-plate configuration, several conditions have to be satisfied, in addition to the recommendations, listed in the previous subsection:

The samples must be cylindrical with parallel upper and lower surfaces. The dimensions of the sample are related to the response of the dynamic shear experiments. The minimal torque, the RFS II is able to detect, is $2 \cdot 10^{-7}$ Nm. To obtain torques in dynamic shear experiments above this minimum, the sample thickness must be minimal and the diameter maximal. The maximal diameter of a sample is limited by anatomical dimensions. The imposed angular displacement must be minimal to avoid geometric nonlinearities. Experiments indicated that samples with a diameter of 10 or 12 mm a thickness of 1–2 mm do yield relevant torques for small displacements.

These samples are prepared in the following manner:
A slice with a thickness in the range 10–20 mm and a diameter of about 20 mm is cut out of the brains with a scalpel. The slice is placed underneath a hollow bore. With this bore a cylinder with a diameter of 10 or 12 mm is cut. The cylinder is embedded in gelatine within a box. This box, together with it's contents, is placed at 7°C in a refrigerator to provide a fast setprocess of the gelatine. On two opposite sides the box is provided with four notches (see fig. C.1). A razor blade is used to cut the samples. It is placed in two opposite notches. With

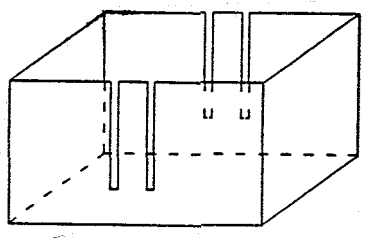

Figure C.1: Box used to prepare samples of brain tissue with a thickness of 1.5–2 mm

small back and forth movements it is pushed through the contents of the box. A second blade is used in the same way and moves through the notches next to the first. Then, the gelatine with it's contents is removed from the box. The gelatine between the razor blades contains the sample that will be used in the experiments. One blade is removed carefully and the sample, still enveloped by the gelatine and stuck to the second blade, is placed in water at 37°C. After the gelatine is dissolved, the sample is removed from the water. The remaining water on the sample is removed with special paper to which the samples do not stick. The sample is placed upon the RFS II between the parallel plates. To centre the samples upon the lower plate, a disc is made with a diameter equal to the lower plate of the RFS II and with a hole in its centre (diameter 10 or 12 mm). The samples are placed in the hole of this plate. Then, the upper plate is carefully lowered to the upper side of the sample. To avoid preshear, the plate is lowered till it's just above the sample. When the plate is lowered further, the normal force upon the upper plate is measured to detect contact between the sample and the upper plate. When the plate touches the sample a tensile force is caused by the surface tension of the liquid between the plate and the sample. If the upper plate is lowered further, this force will decrease. The final distance between the plates is reached when the force, enforced by the moist surface of the samples, has disappeared. The moist chamber is placed and the set up for a measurement is finished.

D Geometrically linear deformations

In section 4.1 it is stated that the enforced deformations are geometrical linear. If $\sin\alpha(t) \approx \alpha(t)$ and if $R\frac{\partial\phi}{\partial z} \gg \left(R\frac{\partial\phi}{\partial z}\right)^2$ then it can be assumed that the deformation is indeed geometrical linear. Typical values for the parameters are listed in table D.1. With these values $\sin\alpha_0 = 2.5 \cdot 10^{-3}$ and $R\frac{\partial\phi}{\partial z} = 0.01$, so both statements are true.

Table D.1: Typical values for torsional shear experiments

Parameter	Typical value
Sample radius	6 mm
Sample height	1.5 mm
Enforced strain	1%
Enforced angular displacement	$2.5 \cdot 10^{-3}$ rad

E Noted information about samples

The donors, used in this project were mainly calves, slaughtered in accordance with islamitic law to prevent defects to the brains. Mostly, the time between sacrifice and start of the preparation was at least 24 hours because the meat has to be inspected. During this time the head of the animal was stored at a temperature of about 7°C. Then the brain were removed and transported in 20 minutes to the university in a expanded polystyrene box with ice. The samples were prepared as described in section C.3.

The results, presented in figure 4.3 to demonstrate the physically linear behaviour of brain tissue are obtained by a sample, consisting of pure white matter. The sample originated from the corona radiata in the left frontal lobe of a calf brain (6 months old). The axis of symmetry of the sample was parallel to the sagittal axis. It was prepared about 27 ± 3 hours after the animal was slaughtered. The radius of the sample was considered to be 11 ± 0.5 mm and it's height equal to 1.50 ± 0.05 mm.

The application of the time/temperature superposition principle was demonstrated with the results of a sample, that consisted of white matter. The sample originated from the left cerebral peduncle, the connection between the left cerebral hemisphere and the pons of a calf brain (6 months old). The axis of symmetry of the sample is parallel to the axis of symmetry of the peduncle. It was prepared 51 ± 3 hours after the animal was slaughtered. The radius of the sample was considered to be 12 ± 0.5 mm and it's height equal to 1.61 ± 0.05 mm.

The principle was also applied to the results, obtained by four other samples. These samples were made by the same sample preparation method and the same donor was used. These samples had the following origin and dimensions (numbering is the same as in table 4.2):

Sample 1 is made from the left side of the calf brain. The cylinder is bored in the midregion. The axis of symmetry was parallel to the transverse axis. The purely white matter sample had a radius of 10 ± 0.5 mm and a height of 1.56 ± 0.05 mm.

Sample 2 is made from the right hemisphere of the calf brain. A cylinder was bored about 60 mm from the forside of the hemisphere, next to the ventricle. The sample consisted of purely white matter. The direction of the axis of symmetry is sagittal. The radius was 11 ± 0.5 mm and the height 1.67 ± 0.05 mm.

Sample 3 is made from the right hemisphere of the calf brain. The cylinder, from which the pure white matter sample is cut, was bored, originated from the backside of the hemisphere, below the backside of the ventricle. The direction of the axis of symmetry made an

angle of 45° with the sagittal plane. The sample had a diameter of 12.0 ± 0.5 mm and an height of 1.80 ± 0.05 mm.

Sample 4 is made from the backside of the right hemisphere, above the ventricle. The symmetry axis of the cylinder was parallel to the transverse axis. The sample consisted of purely white matter and had a radius of 12.0 ± 0.5 mm and a heigth of 1.61 ± 0.05 mm.